



Cite this: *Chem. Soc. Rev.*, 2024, **53**, 3457

Received 12th September 2023

DOI: 10.1039/d3cs00762f

rsc.li/chem-soc-rev

## Recent advances in Rh(I)-catalyzed enantioselective C–H functionalization

Yue Zhang, <sup>†<sup>ab</sup></sup> Jing-Jing Zhang, <sup>†<sup>a</sup></sup> Lujun Lou,<sup>a</sup> Ruofan Lin,<sup>a</sup> Nicolai Cramer, <sup>\*<sup>c</sup></sup> Shou-Guo Wang <sup>\*<sup>d</sup></sup> and Zhen Chen <sup>\*<sup>a</sup></sup>

Chiral carbon–carbon (C–C) and carbon–heteroatom (C–X) bonds are pervasive and very essential in natural products, bioactive molecules, and functional materials, and their catalytic construction has emerged as one of the hottest research fields in synthetic organic chemistry. The last decade has witnessed vigorous progress in Rh(I)-catalyzed asymmetric C–H functionalization as a complement to Rh(II) and Rh(III) catalysis. This review aims to provide the most comprehensive and up-to-date summary covering the recent advances in Rh(I)-catalyzed C–H activation for asymmetric functionalization. In addition to the development of diverse reactions, chiral ligand design and mechanistic investigation (inner-sphere mechanism, outer-sphere mechanism, and 1,4-Rh migration) will also be highlighted.

<sup>a</sup> Jiangsu Co-Innovation Center of Efficient Processing and Utilization of Forest Resources, College of Chemical Engineering, Jiangsu Provincial Key Lab for the Chemistry and Utilization of Agro-Forest Biomass, Jiangsu Key Lab of Biomass-Based Green Fuels and Chemicals, International Innovation Center for Forest Chemicals and Materials, Nanjing Forestry University, Nanjing 210037, Jiangsu, China. E-mail: chenzhen1719@njfu.edu.cn

<sup>b</sup> Jiangsu Key Laboratory for the Research and Utilization of Plant Resources, Institute of Botany, Jiangsu Province and Chinese Academy of Sciences (Nanjing Botanical Garden Mem. Sun Yat-Sen), Nanjing 210014, Jiangsu, China

<sup>c</sup> Institute of Chemical Sciences and Engineering (ISIC), EPFL SB ISIC LCSA, BCH 4305, 1015 Lausanne, Switzerland. E-mail: nicolai.cramer@epfl.ch

<sup>d</sup> Shenzhen Institute of Advanced Technology, Chinese Academy of Sciences, Shenzhen 518055, Guangdong, China. E-mail: shouguo.wang@siat.ac.cn

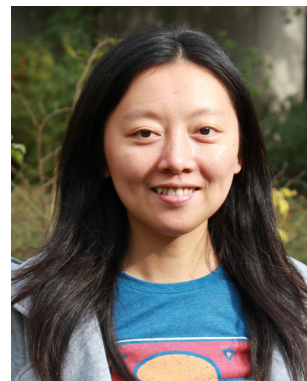
† These authors contributed equally.



**Yue Zhang**

isolation and extraction of natural products from plants and analysis of their biosynthetic pathways.

*Yue Zhang received her BS degree in Chemical Biology in 2015 from Tianjin Normal University (China). She completed her PhD in 2020 under the supervision of Professor Jun-An Ma in Tianjin University (China). Currently, she is an assistant researcher at Institute of Botany, Jiangsu Province and Chinese Academy of Sciences. From 2022 to 2023, she worked as visiting scholar at Nanjing Forestry University. Her research interests focus on chiral synthesis,*



**Jing-Jing Zhang**

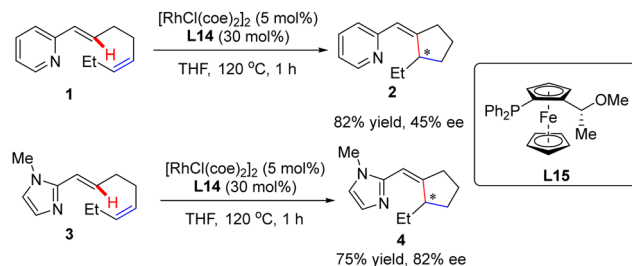
*From 2016 to 2022, she worked as an associate researcher at China Pharmaceutical University. She currently works at Nanjing Forestry University. Her research interests include the design and synthesis of novel compounds with multiple biological activities and the study of the underlying mechanism.*

*Jing-Jing Zhang received her Bachelor's degree in Chemistry and Master's degree in Organic Chemistry from Nanjing University (China) in 2006 and 2009, respectively. Thereafter, she got her PhD degree in Chemical Biology from the University of Hong Kong in 2014 (China). From 2014 to 2016, she worked at Technische Universität Braunschweig (Germany) and Universität Heidelberg (Germany) and was sponsored by Alexander von Humboldt Research Fellowship.*



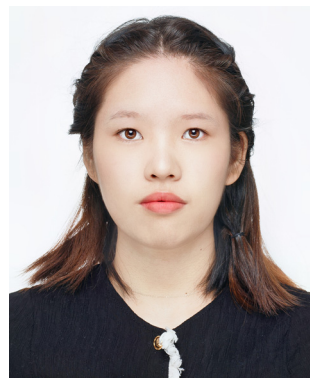
## 1. Introduction

Chiral carbon–carbon (C–C) and carbon–heteroatom (C–X) bonds are pervasive and very essential in natural products, bioactive molecules, and functional materials, and their catalytic construction has emerged as one of the hottest research fields in synthetic organic chemistry.<sup>1–3</sup> Among various methodologies, direct asymmetric functionalization of C–H bonds, which are ubiquitous in organic molecules, *via* transition metal catalysis represents one of the most powerful approaches in this field benefiting from its atom- and step-economy.<sup>4–8</sup> Additionally, such an approach offers a new synthetic opportunity as well as an unconventional and complementary retro-synthetic disconnection compared with traditional methodologies requiring pre-activation or pre-functionalization of both reaction partners. Although C–H bonds are more difficult to be implemented than their pre-functionalized counterparts, they are, virtually, not completely inert, and could be cleaved by an appropriate catalyst to serve as latent surrogates of various functional groups.



**Scheme 1** Rh(I)-Catalyzed enantioselective intramolecular C(sp<sup>2</sup>)–H alkylation of alkenes.

Actually, the past few decades have witnessed the successful implication of diverse transition metals in asymmetric C–H bond functionalization, including first, second, and third-row transition metals, as well as lanthanides.<sup>9–31</sup> Compared to other transition metals, one characteristic feature of rhodium catalysts resides in the availability of multifarious oxidation states (0, 1, 2, and 3), offering an opportunity to effect various catalytic reactions. In particular, rhodium catalysts have been extensively



**Lujun Lou**

*Lujun Lou received her BS degree in Chemical Engineering and Technology in 2023 from Taizhou University. She is now in her first year of postgraduate study under the supervision of Prof. Zhen Chen and Jing-Jing Zhang. Her research interest is the development of catalysis and organofluorine chemistry.*



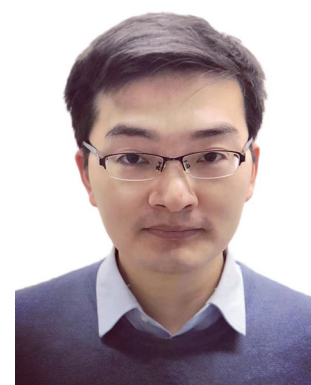
**Ruofan Lin**

*Ruofan Lin received her BS degree in Biology and Medicine in 2021 from Nanjing Forestry University. She is now in her second year of postgraduate study under the supervision of Prof. Zhen Chen. Her research interest is the development of CNS PET ligands and organofluorine chemistry.*



**Nicolai Cramer**

*Nicolai Cramer earned his PhD in 2005 at the University of Stuttgart under the guidance of Sabine Laschat. After a postdoctoral stint with Barry Trost at Stanford, he completed his habilitation at ETH Zurich from 2007 to 2010 with Erick Carreira. Subsequently, he moved to EPFL as assistant professor, was tenured in 2013 and promoted to full professor in 2015. His research encompasses sustainable enantioselective metal-catalyzed transformations and their implementation in synthesis. A focus is placed on asymmetric C–H functionalizations enabled by novel ligand designs.*



**Shou-Guo Wang**

*Shou-Guo Wang obtained his PhD from the Shanghai Institute of Organic Chemistry (SIOC), Chinese Academy of Sciences in 2015 under the supervision of Prof. Shu-Li You before joining the lab Prof. Nicolai Cramer at École Polytechnique Fédérale de Lausanne (EPFL) as postdoctoral researcher. In 2020, he joined the Shenzhen Institutes of Advanced Technology (SIAT), Chinese Academy of Sciences, as a principal investigator. His main research interest encompasses the discovery of new catalytic systems in organic chemistry and beyond to enable their implementation in the synthesis of biologically active molecules.*



investigated in asymmetric C–H functionalization with diverse mechanisms.<sup>32–45</sup> From the viewpoint of substrate activation modes, Rh-catalyzed C–H functionalization could be classified into two categories: inner-sphere mechanism and outer-sphere mechanism, which differ in the mechanism of the C–H activation step (Scheme 1).<sup>46,47</sup> Generally, Rh(III)-catalyzed asymmetric C–H functionalization adopts the inner-sphere mechanism by taking advantage of a chiral cyclopentadienyl (Cp) ligand,<sup>35,38,39,48–51</sup> whereas Rh(II) usually coordinates with a chiral carboxylic acid to achieve the effect of asymmetric C–H functionalization *via* the outer-sphere mechanism,<sup>14,52–54</sup> both of which have been well reviewed elsewhere.

Of note, the last decade has witnessed vigorous progress in Rh(I)-catalyzed asymmetric C–H functionalization as a complement to Rh(II) and Rh(III) catalysis. In the asymmetric Rh(I) catalysis, both inner-sphere and outer-sphere mechanisms could be involved, despite that the inner-sphere dominates (Fig. 1). Additionally, a special 1,4-Rh migration pathway may also be involved in the asymmetric Rh(I) catalysis. Notably, various types of chiral ligands could be implemented including phosphoramidite, phosphonate, carbodicarbene, bisoxazoline-phosphane, BINAP, Segphos, Tangphos, Josiphos, diene, and so on (Fig. 2). As a consequence, a diversity of asymmetric C–H transformations, such as alkylation, alkenylation, allylation, arylation, and silylation, have been developed. Despite these advances, a review comprehensively summarizing Rh(I)-catalyzed asymmetric C–H functionalization is elusive. Herein, we aim to provide the most comprehensive and up-to-date summary covering the recent advances in Rh(I)-catalyzed asymmetric functionalization of both C(sp<sup>2</sup>)-H and C(sp<sup>3</sup>)-H bonds. Rh(I)-catalyzed hydroacylations and Friedel–Crafts reactions have been the subject of multiple reviews and are therefore not covered here.<sup>55,56</sup> We believe that this review will gain much attention from researchers with C–H functionalization and asymmetric transition metal catalysis backgrounds, stimulate

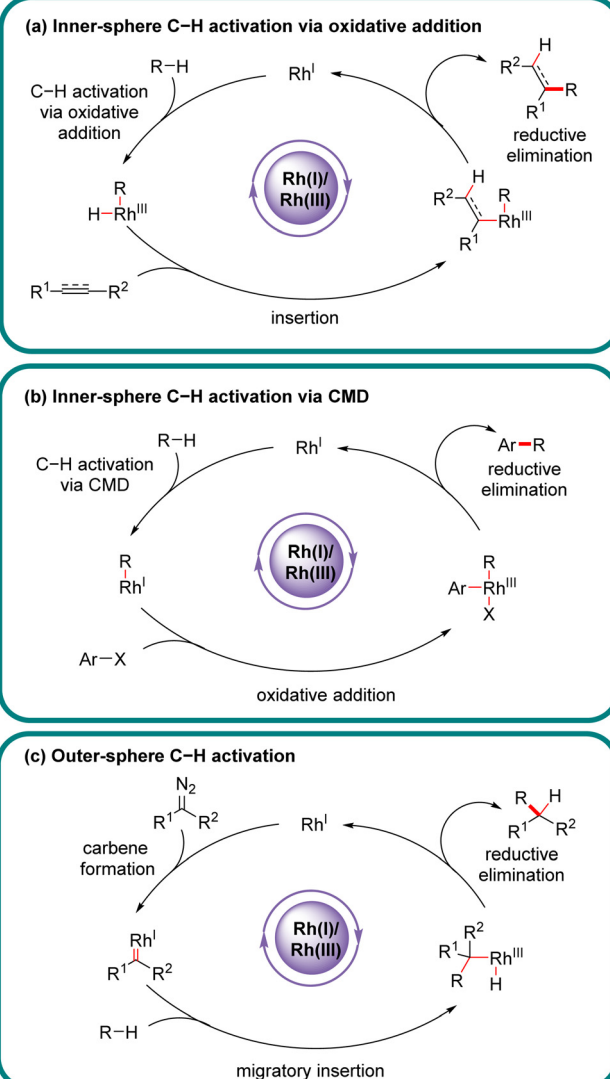


Fig. 1 Catalytic cycles for Rh(I)-catalyzed enantioselective C–H functionalization.



Zhen Chen

Zhen Chen received his BS degree in Applied Chemistry in 2013 from Tianjin University (China). He completed his PhD in 2019 under the supervision of Prof. Jun-An Ma at Tianjin University (China). From 2017 to 2020, he studied radiochemistry as an exchange PhD student and postdoctoral fellow with Prof. Steven H. Liang at Harvard Medical School/Massachusetts General Hospital (HMS/MGH, USA). From 2020 to 2021, he

worked as a postdoctoral research fellow in the group of Prof. Nicolai Cramer at EPFL (Switzerland). Currently, he is a full professor at Nanjing Forestry University. His research interests focus on the development of novel catalytic synthetic methodologies and PET biomarkers.

more future efforts in this area, and facilitate the synthetic application of these novel reactions. We have structured the literature according to substrate activation modes and reaction types.

## 2. Inner-sphere C–H functionalization

In the inner-sphere mechanism, the metal directly interacts with a specific C–H bond to effect its activation and cleavage, leading to a discrete organo-rhodium species to proceed with follow-up functionalization. For Rh(I)-catalyzed asymmetric C–H functionalization, the inner-sphere mechanism represents the most prevalent C–H activation pathway. Owing to the fundamental differences in substrate activation modes, the selectivity of multiple C–H bonds differs. Typically, the inner-sphere activation mode is highly sensitive to the steric factor surrounding C–H bonds.



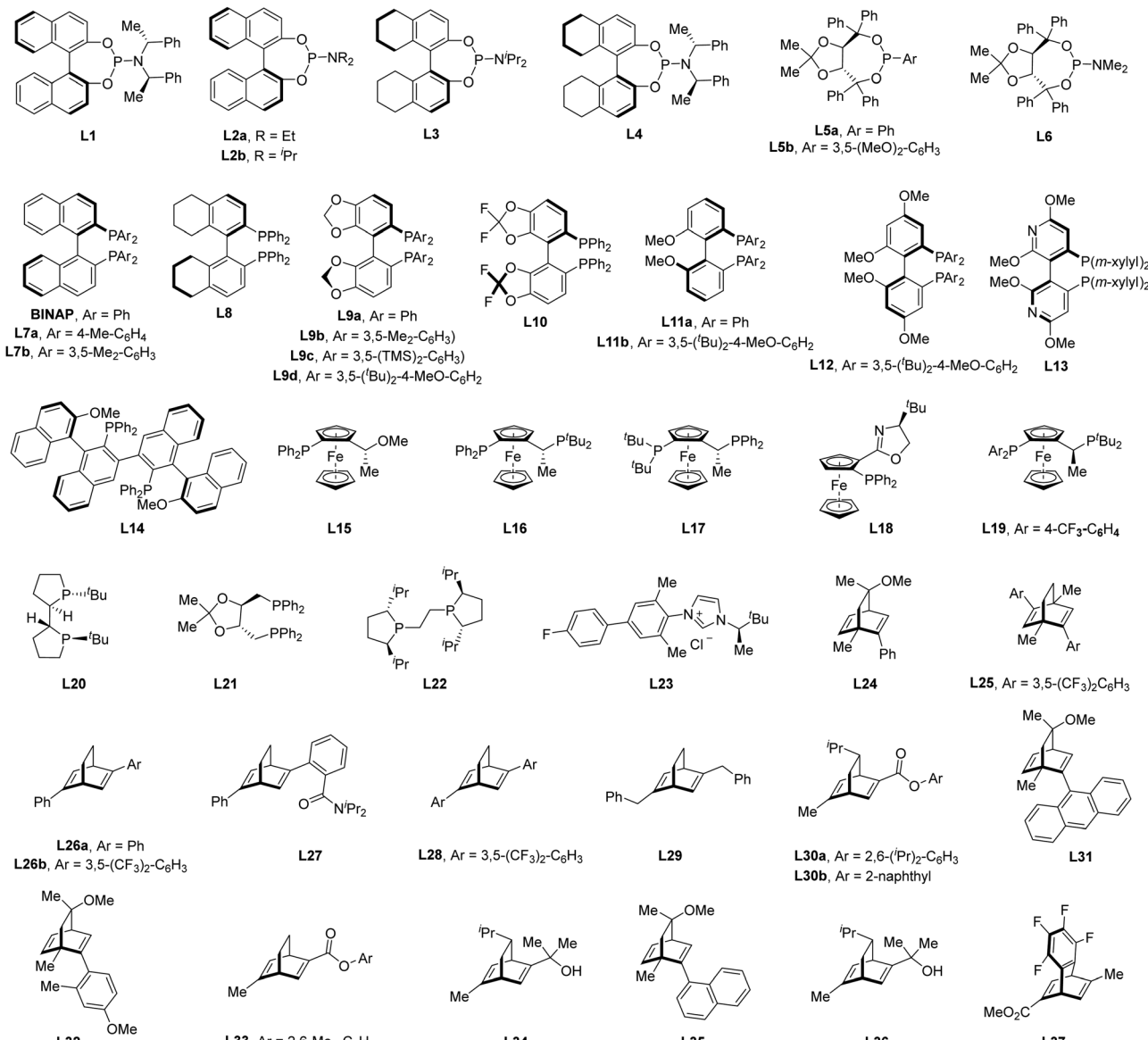


Fig. 2 The generally used chiral ligands in Rh(i)-catalyzed asymmetric C–H functionalization.

## 2.1 Functionalization of C(sp<sup>2</sup>)-H bonds

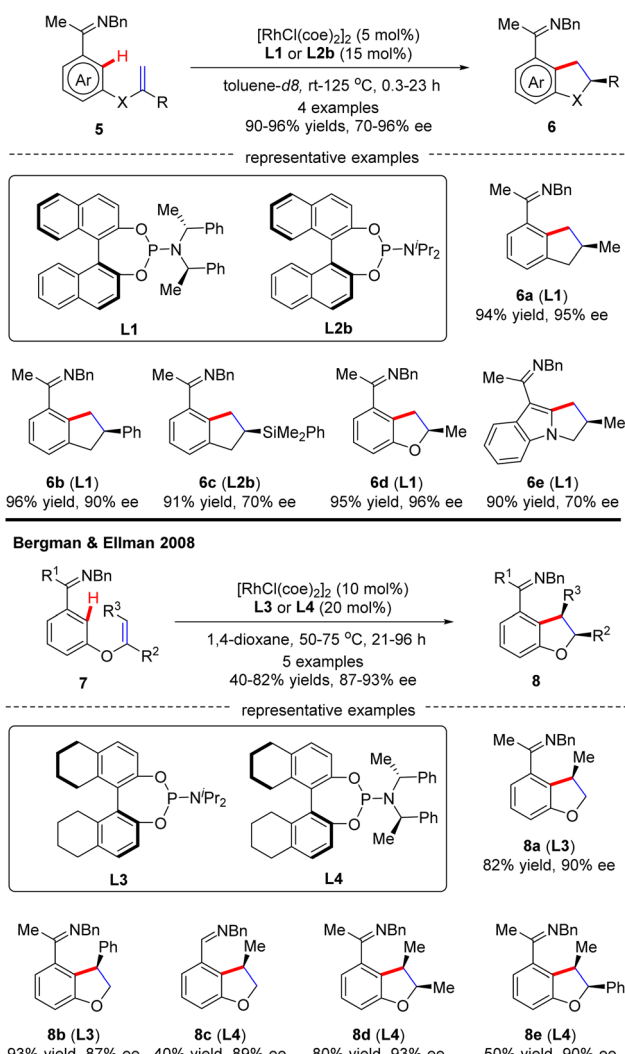
Compared with C(sp<sup>3</sup>)-H bonds, the sp<sup>2</sup>-hybridized counterparts are generally more sterically accessible and acidic, leading to more vigorous progress in C(sp<sup>2</sup>)-H functionalization. Additionally, rhodium usually possesses a good coordination affinity to unsaturated double and triple C–C bonds. Therefore, the use of alkenes, allenes, or alkynes as electrophiles can provide a good solution for the Rh(i)-catalyzed asymmetric functionalization of C(sp<sup>2</sup>)-H bonds.

**2.1.1 Asymmetric addition of C(sp<sup>2</sup>)-H bonds to unsaturated bonds.** In this part, Murai and co-workers pioneered a Rh(i)-catalyzed asymmetric intramolecular alkene C(sp<sup>2</sup>)-H activation/olefin coupling reaction of 1,5-dienes with a 2-pyridyl (1) or 2-imidazolyl (3) directing group in 1997 (Scheme 1).<sup>57</sup> By the use of monodentate planar chiral ferrocene phosphine ligand L15, the desired cyclopentane derivatives 2 and 4 were attained in 45% and

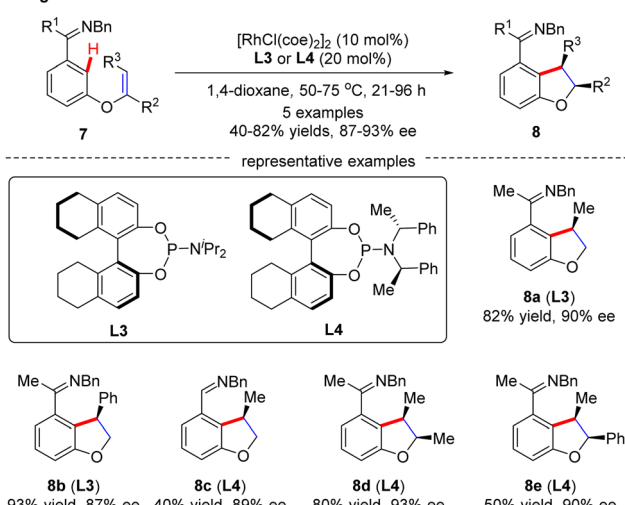
82% ee, respectively. Following this pioneering work, an elegant example was communicated at the beginning of this century, when Bergman and Ellman effected an imine-directed intramolecular addition of aromatic C–H bonds to 1,1-disubstituted alkenes (Scheme 2).<sup>58</sup> Using [RhCl(coc)<sub>2</sub>]<sub>2</sub> as the catalyst and (S)-binaphthol (BINOL)-derived monodentate phosphoramidite L1 or L2b as the chiral ligand, several five-membered carbo- and heterocycles 6 were accessed with impressive yields and enantioselectivities (up to 96% yield and 96% ee). Subsequently, the same group further expanded the substrate scope to 1,2-disubstituted as well as 1,1,2-trisubstituted alkenes by taking advantage of (S)-octahydrobinaphthol-based phosphoramidite L3 as a chiral ligand, thus giving rise to 2,3-dihydrobenzofuran derivatives 8 in moderate to excellent yields (40–82%) and excellent enantioselectivities (87–93% ee).<sup>59</sup> For the cyclization of aldimine or 1,1,2-trisubstituted alkene substrates, ligand L4 provided better



Bergman &amp; Ellman 2004

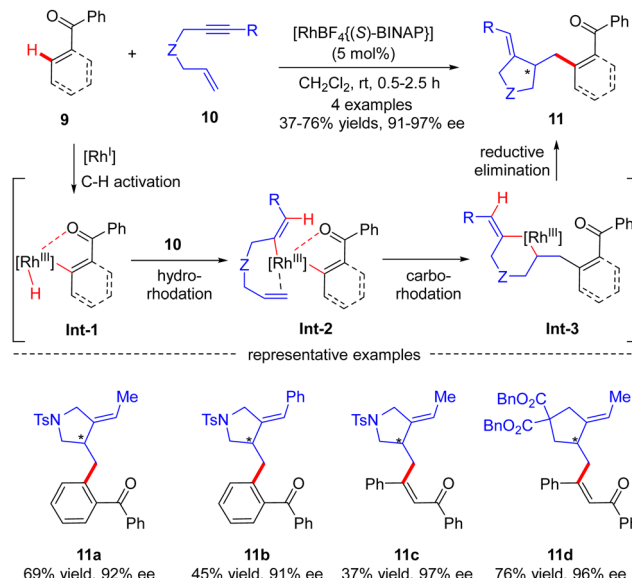


Bergman &amp; Ellman 2008

Scheme 2 Rh(I)-Catalyzed enantioselective imine-directed intramolecular  $C(sp^2)$ -H alkylation.

enantiocontrol. Notably, only *syn*-selective products were achieved, owing to that the *E*-alkenes, which would lead to *anti*-selective products, were unreactive. More importantly, the application of this approach was validated by the total synthesis of a PKC inhibitor.<sup>60</sup>

Aside from several reports of imine-directed  $C(sp^2)$ -H functionalization, carbonyl could also serve as an effective directing group to enable similar transformations. For example, in 2007, Shibata and co-workers described a carbonyl-directed cascade  $C(sp^2)$ -H activation and cyclization with enynes *via* asymmetric Rh(I) catalysis.<sup>61</sup> With the chiral Rh-(*S*)-BINAP complex as a catalyst, both alkyl and aryl substituted *N*-tethered enynes readily reacted with the  $C(sp^2)$ -H bond of benzophenone to furnish products **11a** and **11b** with 92% and 91% ee, respectively (Scheme 3). Apart from benzophenone, vinylic C-H functionalization of chalcone was also effected, thus affording the corresponding dienones **11c** and **11d** in excellent enantioselectivities. For the mechanism, the reaction was speculated to commence with carbonyl-directed C-H oxidative addition onto

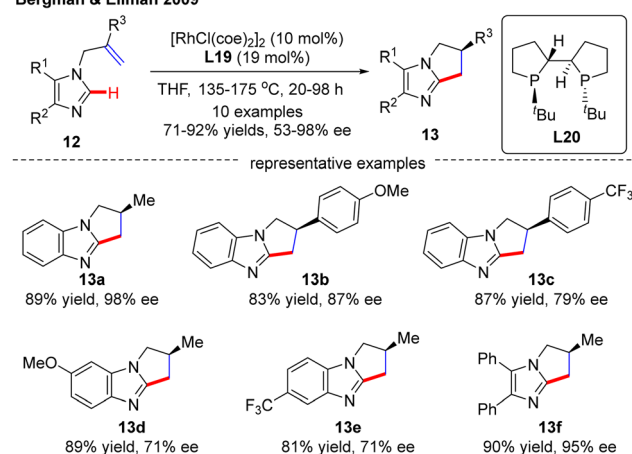


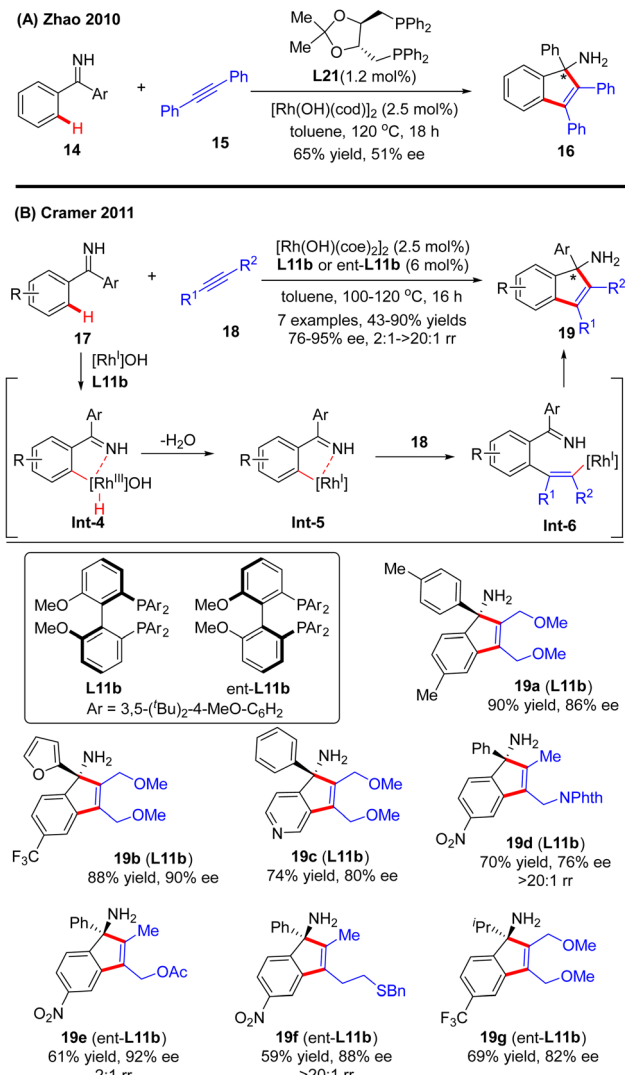
Scheme 3 Rh(I)-Catalyzed cyclization of enynes initiated by carbonyl-directed activation of aromatic and vinylic C-H bonds.

Rh(I) to provide aryl- or alkanyl-rhodium complex **Int-1**. Hydro-rhodation of **Int-1** to the alkyne moiety of enyne **10** afforded intermediate **Int-2**, which then underwent intramolecular carbo-rhodation to the alkene moiety to afford metallacyclohexane **Int-3**. Finally, reductive elimination of **Int-3** led to the release of the desired product **11**.

In 2009, Bergman and Ellman documented a Rh(I)-catalyzed intramolecular asymmetric  $C(sp^2)$ -H alkylation of imidazoles (Scheme 4).<sup>62</sup> While most bidentate ligands failed to deliver the desired product according to their previous work,<sup>63</sup> Tangphos (**L20**) represented an exception. At elevated temperatures (135-175 °C), the intramolecular cyclization of allyl-substituted imidazoles **12** readily proceeded to forge various dihydro-pyrrolo-imidazoles **13** in moderate to excellent yields (71-92%) and enantioselectivities (53-98% ee).

Bergman &amp; Ellman 2009

Scheme 4 Rh(I)-Catalyzed enantioselective intramolecular  $C(sp^2)$ -H alkylation of imidazoles.

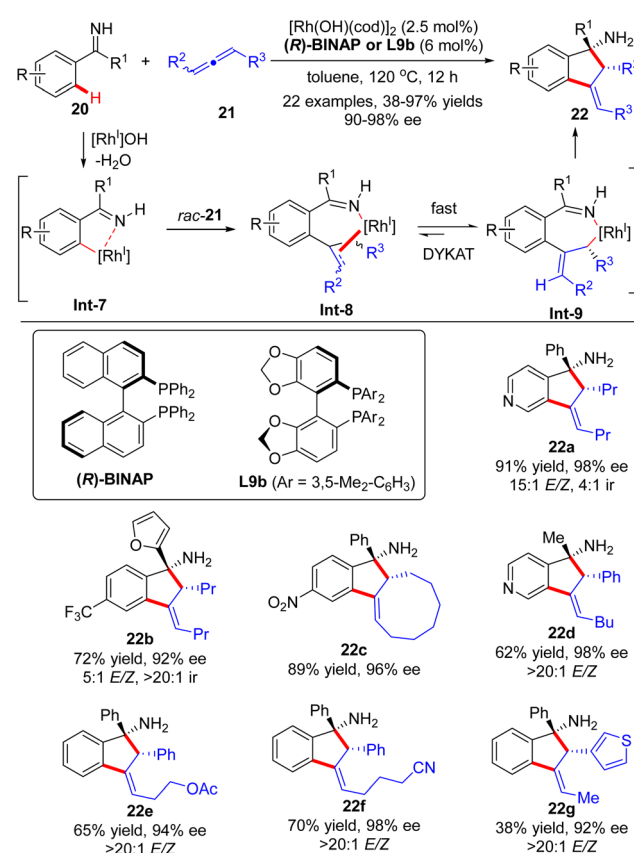


Scheme 5 Rh(i)-Catalyzed [3+2] annulations of aromatic ketimines with internal alkynes.

In 2010, Zhao and co-workers reported a single example of a Rh(i)-catalyzed [3+2] annulation reaction of benzophenone imine **14** with diphenylacetylene **15**.<sup>64</sup> In this reaction, the imine group in benzophenone imine **14** not only served as a directing group to enable C(sp<sup>2</sup>)-H activation at the *ortho*-position, but also could be transformed into an amino group by an addition reaction across the C=N bond. To their disappointment, with bidentate phosphine (*R,R*)-DIOP **L21** as the chiral ligand, only moderate enantioselectivity (51% ee) was achieved for the production of the tertiary 1*H*-inden-1-amine **16**. Subsequently, the Cramer group disclosed an elegant approach for the [3+2] annulation reaction of aromatic ketimines **17** with internal dialkyl or arylalkyl alkynes **18** by taking advantage of the biphenyl diphosphine ligand DTBM-MeOBiphep (**L11b**) (Scheme 5).<sup>65</sup> This approach allowed for the synthesis of a broad set of tertiary 1*H*-inden-1-amine derivatives **19** in 43–90% yields and good to excellent enantioselectivities (76–95% ee). The reaction was envisioned to be

initiated by imine-directed *ortho* C(sp<sup>2</sup>)-H activation to form the cyclometalated rhodium complex **Int-4**. Notably, the C(sp<sup>2</sup>)-H activation step revealed a good positional preference for the more electron-poor aromatic substituent of the ketimine substrates. Subsequent removal of hydrogen from the metal center in **Int-4** provided intermediate **Int-5**, which was essential to avoid undesirable hydroarylation reactivity. Migratory insertion of **Int-5** into internal alkyne **18** then occurred to furnish an alkenyl-rhodium species **Int-6**, wherein the regioselectivity control could be achieved by using a potentially coordinating functional group in unsymmetrically substituted alkynes, such as ether (**19a–c**, **19g**), ester (**19e**), phthalimide (**19d**), and sulfur-containing group (**15f**). Finally, enantioselective addition of **Int-6** across the ketimine group set the desired product **19**.

Soon after, the Cramer group further devised a Rh(i)-catalyzed dynamic kinetic asymmetric transformation (DYKAT) of racemic allenes **21** with ketimines **20** (Scheme 6).<sup>66,67</sup> Similar to the above-described process with alkynes, this [3+2] annulation version of allenes with ketimines exhibited excellent regio-selectivity ranging from 4 : 1 (**22a**) to >20 : 1 (**22b**). The regio-selectivity resulted from the different positions of C-H activation of ketimines, which favored the electron-poor aryl and heteroaryl substituents. The coordination and migratory insertion of the initially generated cyclometalated species **Int-7** into a racemic allene **21** gave rise to eight stereoisomers **Int-8**,

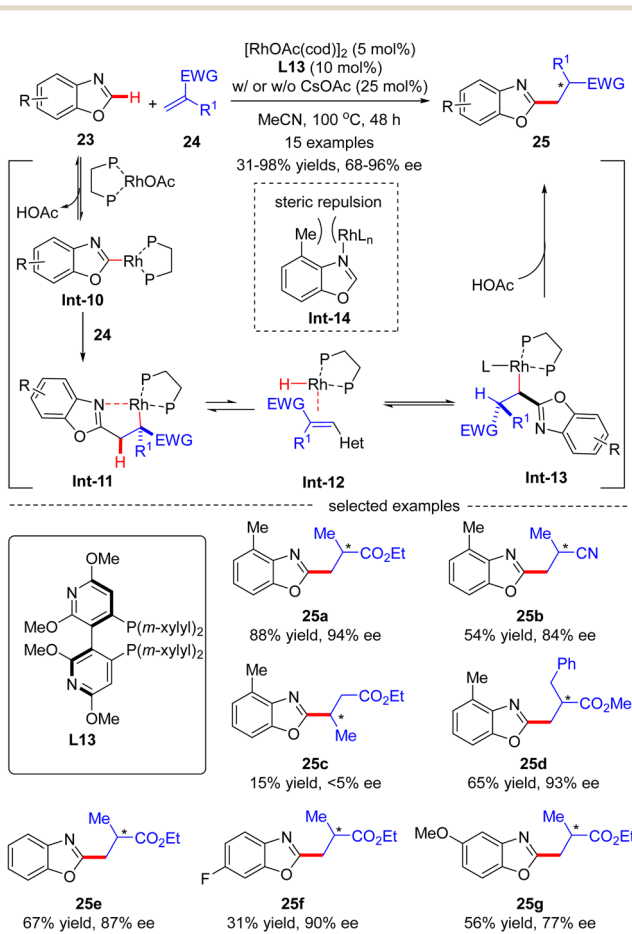


Scheme 6 Rhodium(i)-Catalyzed [3+2] annulations of aromatic ketimines with allenes.



which rapidly equilibrated and isomerized to reach the appropriate (*E*)-allyl isomer **Int-9** by either a  $\beta$ -H elimination/re-addition sequence or a  $\sigma$ - $\pi$ - $\sigma$  mechanism.<sup>68</sup> Follow-up intramolecular 1,2-addition across the imine moiety in **Int-9** prevailed to arrive at the desired indanylamine **22** with excellent diastereomeric (*syn*-diastereoselectivity) and enantiomeric control (90–98% ee). For unsymmetrically 1,3-disubstituted allenes, the selectivity in the equilibration process of **Int-8** was intensively governed by electronic factors with a preference for the formation of a benzylic allyl rhodium intermediate over the alternative alkyl allyl intermediate. Notably, the ketimine part did not exert a significant effect on the enantioselectivity, and both aryl aryl and aryl alkyl ketimines were well suited for this reaction.

In 2015, Rovis and co-workers disclosed an asymmetric intermolecular  $C(sp^2)$ -H alkylation of benzoxazole **23** with acrylates **24** *via* Rh(i)-catalysis (Scheme 7).<sup>69</sup> Mechanistic studies indicated that this reaction was initiated by reversible  $C$ -H activation of benzoxazole **23** with the aid of the rhodium acetate catalyst, thus providing Rh-benzoxazole complex **Int-10**. Migratory insertion of **Int-10** across acrylate **24** furnished Rh-enolate **Int-11**, which isomerized into heterobenzylic rhodium species **Int-13** *via* a  $\beta$ -hydride elimination/hydrorhodation sequence. Protonation of **Int-13** then occurred to set the alkylated benzoxazole **25**, which was assumed to be the turnover limiting step. It



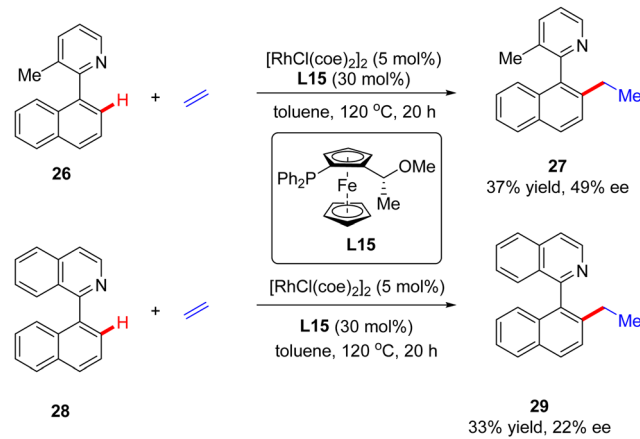
Scheme 7 Rh(i)-Catalyzed asymmetric intermolecular  $C(sp^2)$ -H alkylation of benzoxazoles with acrylates.

was also demonstrated that 4-methylbenzoxazole, characteristic of a [1,3]-strain, disfavored strong coordination to rhodium in **Int-14**, thus exhibiting higher reactivity compared with its 6-substituted or unsubstituted counterparts (**25a** *vs.* **25e** *vs.* **25f**). In this scenario, the authors took advantage of a bulky Segphos derivative CTH-(*R*)-Xylyl-P-Phos (**L13**) as chiral ligand to surmount the possible deleterious coordination of the heteroarene and harness the reactivity. As a consequence, a diversity of 2-alkylated benzoxazoles **25** were attained in moderate to excellent yields (31–98%) and good to excellent enantioselectivities (68–96% ee). This reaction was tolerant of  $\alpha$ -methyl substituted acrylate derivatives, whereas using  $\beta$ -substituted acrylate derivative crotonate as an alkylation reagent led to the racemic product **25e** in extremely poor results (15% yield and <5% ee).

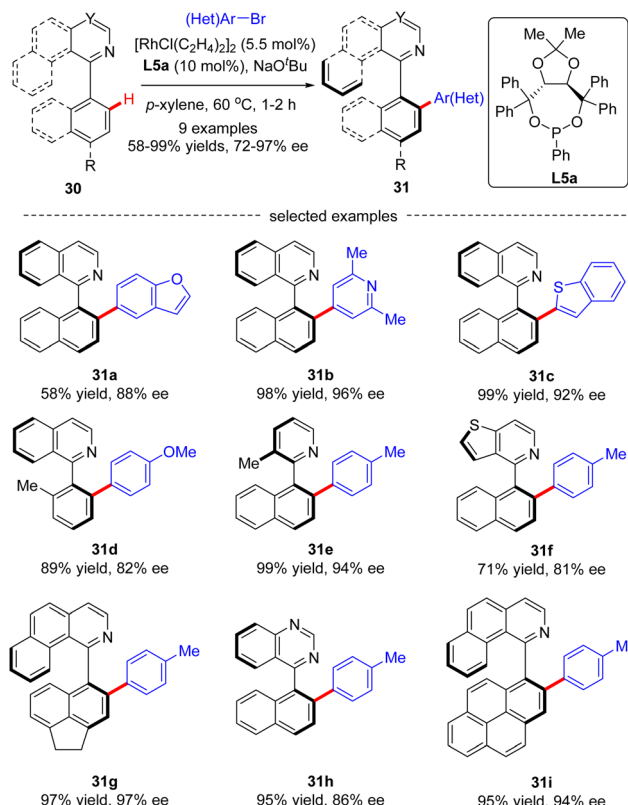
In addition to a number of reports on constructing central chirality, Rh(i)-catalyzed addition of  $C(sp^2)$ -H to unsaturated bonds could also be applied in effecting axial chirality. In 2000, Murai and co-workers, for the first time, disclosed the construction of axially chiral biaryls **27** and **29** *via* Rh(i)-catalyzed  $C(sp^2)$ -H alkylation of naphthylpyridine derivatives **26** & **28** with ethylene (Scheme 8).<sup>70</sup> Unfortunately, only moderate yields and enantioselectivities could be achieved (up to 37% yield and 49% ee) with  $[\text{RhCl}(\text{cod})_2]$  as the catalyst and chiral ferrocenyl phosphine **L15** as the ligand.

**2.1.2 Asymmetric arylation of  $C(sp^2)$ -H bonds.** In 2019, You and co-workers reported a Rh(i)-catalyzed atroposelective  $C(sp^2)$ -H arylation of heterobiaryls **30** with aryl and heteroaryl bromides (Scheme 9).<sup>71</sup> By taking advantage of TADDOL-derived monodentate phosphonite **L10** as the chiral ligand and *N*-heterocycles as directing groups, a diverse set of axially chiral heterobiaryls **31** were released in moderate to excellent yields (58–99%) with high to excellent enantioselectivities (72–99% ee). Remarkably, this approach lays a foundation to synthesize various axially chiral heterobiaryl catalysts.

Recently, the implementation of planar chirality in Rh(i)-catalyzed  $C(sp^2)$ -H functionalization was also demonstrated by You and co-workers (Scheme 10A).<sup>72</sup> With thioketone as the directing group and **L5a** as the chiral ligand, a range of aryl and



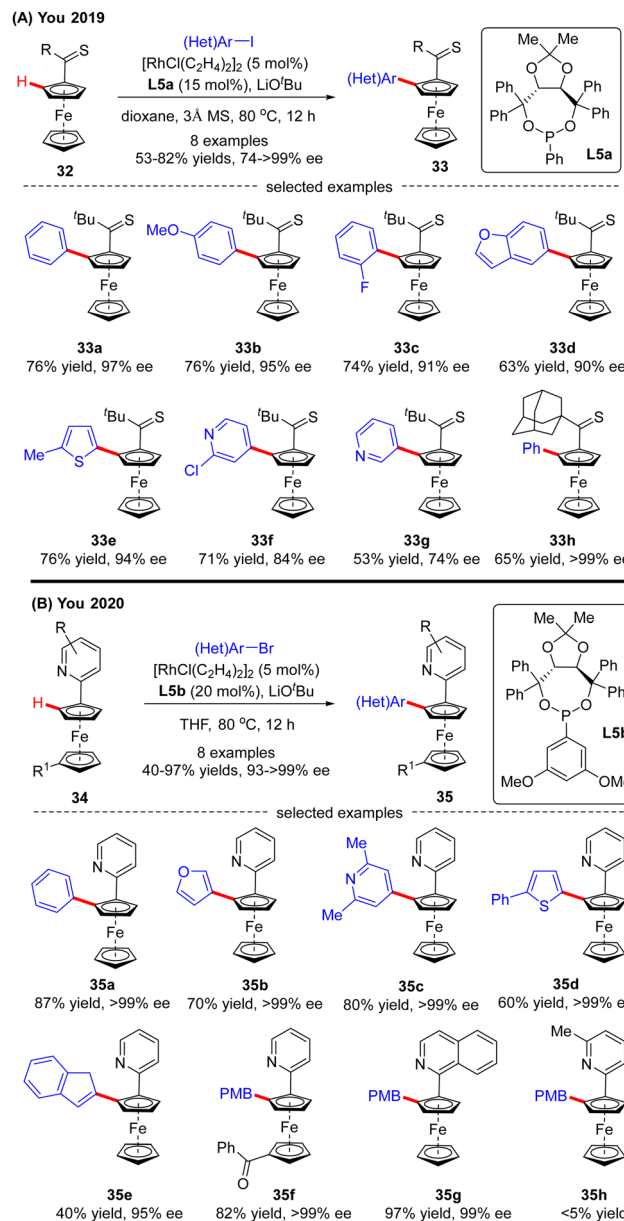
Scheme 8 Rh(i)-Catalyzed atroposelective  $C(sp^2)$ -H alkylation of naphthylpyridine derivatives with ethylene.



**Scheme 9**  $\text{Rh}(\text{i})$ -Catalyzed atroposelective  $\text{C}(\text{sp}^2)\text{-H}$  arylation of heterobiaryls with aryl and heteroaryl bromides.

heteroaryl iodides were readily incorporated into thiocarbonyl-ferrocene **32**, thus providing direct access to various planar chiral ferrocenes **33** in moderate to good yields (53-82%) and excellent enantioselectivities (up to >99% ee). Subsequently, the same group further extended the ferrocene scope to pyridylferrocenes **34** by use of the  $\text{Rh}(\text{i})$ /phosphonite catalytic system, wherein pyridine served as the directing group (Scheme 10B).<sup>73</sup> As a consequence, a variety of (hetero)aryl bromides were readily coupled with pyridylferrocenes **34** to afford planar chiral ferrocene-based pyridine derivatives **35** in excellent yields (up to 97%) and enantioselectivities (93->99% ee). Additionally, aryl iodide and aryl chloride were competent coupling partners, leading to the formation of **35a** in comparable results (95% and >99% ee, respectively). Notably, aside from (hetero)aryl halides, alkenyl bromide also proved compatible with this reaction, giving product **35e** in 40% yield and 95% ee. Meanwhile, substitution on the pyridine ring or ferrocene part was also tolerated (**35f**, **35g**). However, 5-substituted pyridine was not a suitable substrate, which was probably attributed to its weak coordination with the rhodium catalyst (**35h**).

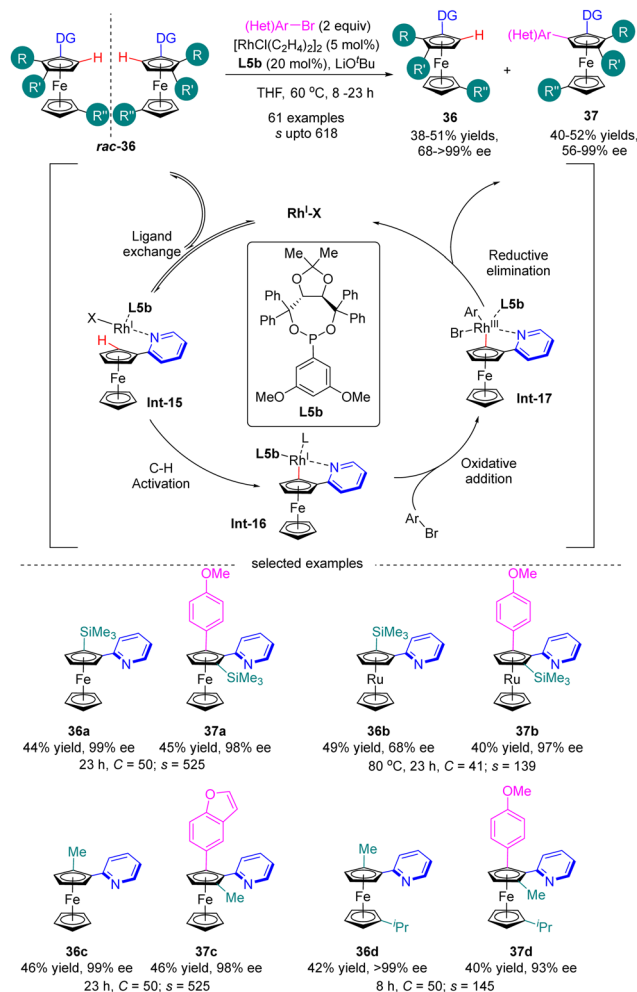
Most recently in 2023, You and co-workers further achieved the  $\text{Rh}(\text{i})$ -catalyzed enantioselective  $\text{C}(\text{sp}^2)\text{-H}$  arylation of metallocenes for the synthesis of both planar chiral 1,2-disubstituted and 1,3-disubstituted metallocenes *via* kinetic resolution (Scheme 11).<sup>74</sup> In the presence of  $\text{Rh}(\text{i})$  catalyst and 3,5-( $\text{MeO}$ )<sub>2</sub> $\text{C}_6\text{H}_3$ -substituted TADDOL-derived monodentate phosphonite



**Scheme 10**  $\text{Rh}(\text{i})$ -Catalyzed enantioselective  $\text{C}(\text{sp}^2)\text{-H}$  functionalization of ferrocenes (PMB = *p*-methoxybenzyl).

**L5b** as the chiral ligand, a broad range of aryl and heteroaryl bromides were readily incorporated into various directing group (*e.g.* 3- or 4-methyl, 4-phenyl and 4-methoxy pyridine) functionalized 1,2-disubstituted or 1,3-disubstituted ferrocenes and ferrocenes *rac*-**36** containing diverse substituents, including alkyl groups, aryl groups, and even heteroatoms, thus giving rise to arylated products **37** with satisfactory selectivity factor values (*s* up to 618) and excellent enantiomeric control (up to 99% ee). For instance, ferrocene **36a** and ruthenocene **36b** with *ortho*-trimethylsilyl substituent acted as applicable substrates with outstanding selectivity (*s* = 525 for **37a** and *s* = 139 for **37b**). Additionally, the calculated conversion (*C*) matched well with the isolated yields. The underlying mechanism of this reaction has been studied using 2-pyridinylferrocenes and aryl bromides as

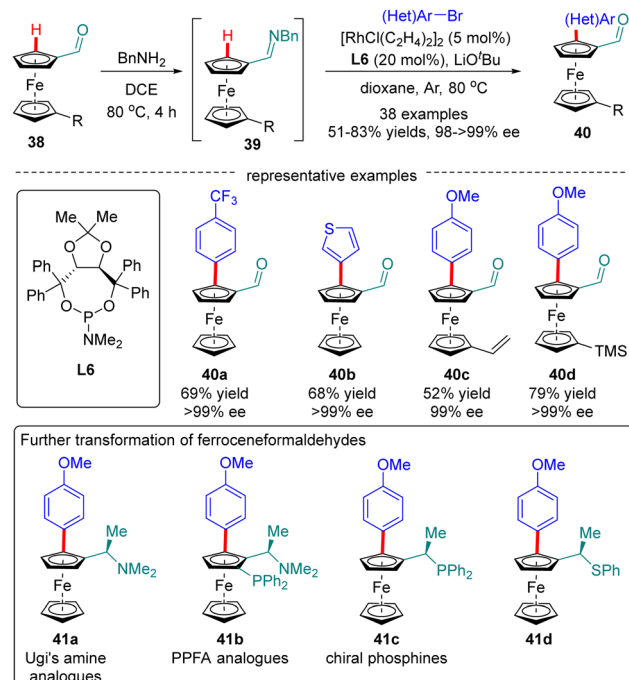




Scheme 11 Rh(I)-Catalyzed enantioselective C(sp<sup>2</sup>)-H arylation of metallocenes via kinetic resolution.

representative reagents by both experimental and computational studies (Scheme 11).<sup>75</sup> The reaction was proposed to be initiated by the coordination of rhodium with 2-pyridinylferrocenes to afford intermediate **Int-15**. Subsequently, C-H activation of **Int-15** occurred to generate intermediate **Int-16**, which then proceeded to oxidative addition with aryl bromide to provide **Int-17**. Finally, reductive elimination of **Int-17** readily proceeded to arrive at the expected product and release the rhodium catalyst.

Ferroceneformaldehydes constitute a vital type of platform molecules, which can be smoothly converted into diverse functionalities to provide facile access to chiral ligands and catalysts. However, it had been a long-standing challenge to synthesize enantiopure planar chiral ferroceneformaldehydes *via* a straightforward and highly efficient approach. To surmount this obstacle, You and co-workers recently disclosed a Rh(I)-catalyzed enantioselective C(sp<sup>2</sup>)-H arylation of ferroceneformaldehydes **38** with the assistance of a chiral phosphoramidite ligand **L6** (Scheme 12).<sup>76</sup> It was demonstrated that the formation of imine intermediates **39** was critical for the success of this transformation. A broad set of readily available aryl halides such as aryl iodides, aryl bromides, and even aryl

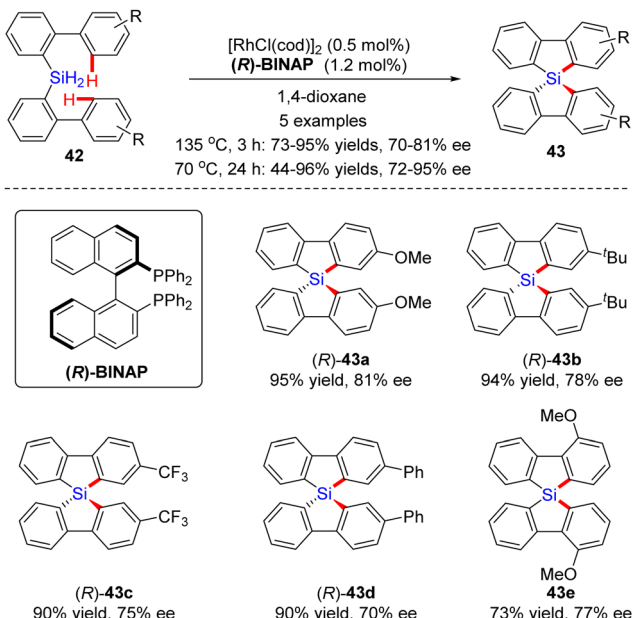


Scheme 12 Rh(I)-Catalyzed enantioselective C(sp<sup>2</sup>)-H arylation of ferroceneformaldehydes.

chlorides are found to be competent substrates for this reaction, providing access to chiral ferroceneformaldehydes **40** in uniformly excellent enantioselectivity (98->99% ee). Among various functionalities derived from ferroceneformaldehydes by an elegant decoration of the aldehyde group, enantiopure Ugi's amine **41a** and PPFA analogues **41b** were particularly noteworthy, as the latter proved as a highly efficient ligand in Pd-catalyzed asymmetric allylic alkylation reactions.

**2.1.3 Asymmetric silylation of C(sp<sup>2</sup>)-H bonds.** In 2013, Takai and collaborators presented a Rh(I)-catalyzed dual dehydrogenative cyclization of bis(biphenyl)silanes **42** *via* C-H silylation (Scheme 13).<sup>77,78</sup> By the use of [RhCl(cod)]<sub>2</sub> as a catalyst and (R)-BINAP as a ligand, several chiral spirosilabifluorenes **43** were constructed in favorable yields (73-85%) and enantiomeric control (70-81% ee). Subsequently, the same group found that the enantioselectivities of the products could be further enhanced to 72-95% ee without sacrificing the yields by lowering the temperature from 135 °C to 70 °C and extending the reaction time to 24 h.<sup>79</sup>

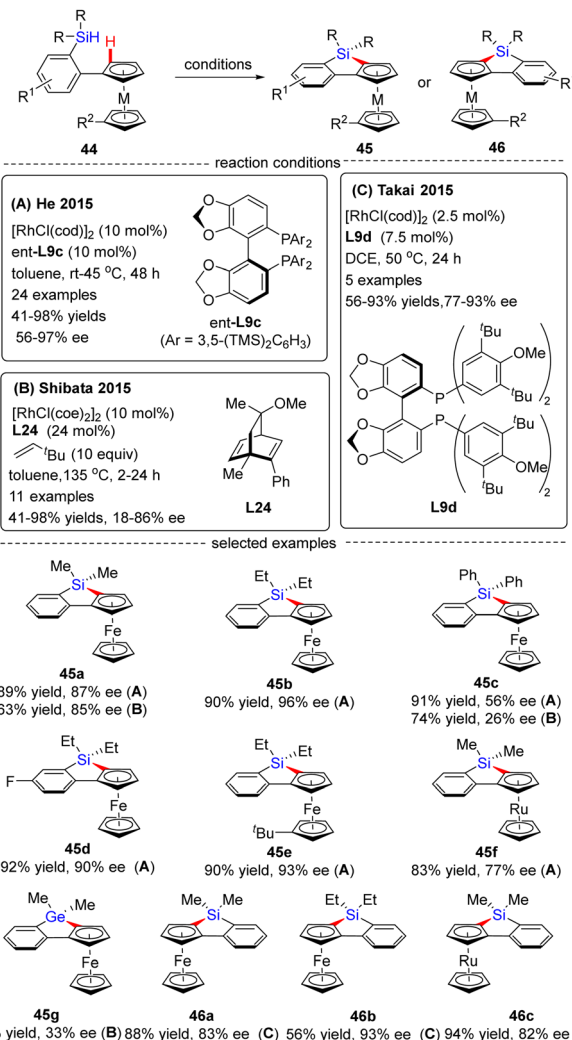
In 2015, He and co-workers opened the door to the untamed Rh(I)-catalyzed asymmetric C-H bond silylation under much milder reaction conditions (Scheme 14A).<sup>80</sup> With the aid of chiral ligand (S)-TMS-Segphos (*ent*-**L9c**), a plethora of Fe and Ru metallocenes **44** proceeded intramolecular dehydrogenative cyclization at temperatures between room temperature and 45 °C, thus providing direct access to planar-chiral ferrocene and ruthenocene siloles **45** in good yields (up to 98%) with high to excellent enantioselectivities (up to 97% ee). In general, the enantioselectivity was largely independent of the substituents on the aryl or metallocene part. In contrast, the substituents on the silicon atom exerted a profound effect on the enantioselectivity,



**Scheme 13** Rh(i)-Catalyzed dual dehydrogenative cyclization of bis(biphenyl)silanes.

and substrates with two ethyl or propyl groups on the silicon atom gave rise to better results (**45b**) compared with that with two methyl groups (**45a**). Besides, only moderate enantiocontrol (56% ee) was achieved for diphenyl silane **45c**. Meanwhile, the Takai group realized the same transformation by using (*R*)-DTBM-Segphos **L9d** as a chiral ligand, which provided several planar-chiral ferrocene and ruthenocene siloles **46** in comparable enantioselectivities (77–93% ee) but with opposite absolute configuration (Scheme 14C).<sup>81,82</sup> Remarkably, apart from Segphos-derived ligand, a chiral diene ligand **L24** was also competent to effect this transformation, but with much lower yields (39–75%) and enantioselectivities (18–86% ee), as described by Shibata and co-workers (Scheme 14B).<sup>83</sup> Additionally, this catalytic system was also applied for the intramolecular dehydrogenative coupling of the C(sp<sup>2</sup>)-H bond with the Ge-H bond in (dimethylhydrogermyl)phenylferrocene **45g**. Unfortunately, the corresponding benzogermoloferrocene **45g** was afforded with only 40% yield and 33% ee. It should be noted that an excess of 3,3-dimethylbut-1-ene as additive was crucial for the maintenance of enantiocontrol.

In 2020, He and co-workers developed a Rh(i)-catalyzed cascade enantioselective C(sp<sup>2</sup>)-H silylation/alkene hydroxilylation of dihydrosilanes (Scheme 15).<sup>84</sup> By the use of Josiphos-derived chiral ligand **L16**, a diverse set of bi-(hetero)aryl dihydrosilanes **47** with different substituents at different positions were smoothly converted to silicon-stereogenic tetrasubstituted silanes **48** in 55–88% yields and good to excellent enantiocontrol (81–99% ee). For the scope of alkene partners, alkyl, aryl and heteroatom-substituted alkenes all proved as competent substrates. Alternatively, with (*R*)-Segphos as a chiral ligand, various ferrocene dihydrosilanes **49** were compatible with this transformation, which enabled streamlined construction of tetrasubstituted silicon-stereogenic and planar

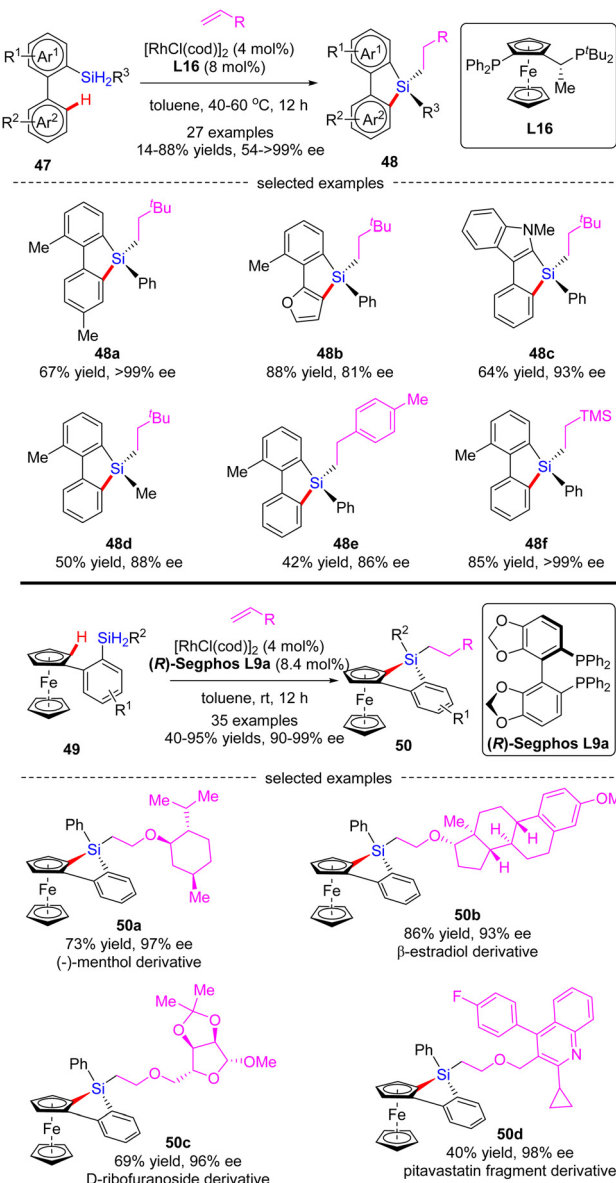


**Scheme 14** Rh(i)-Catalyzed enantioselective intramolecular C-H silylation for the synthesis of planar-chiral metallocene siloles and germolane.

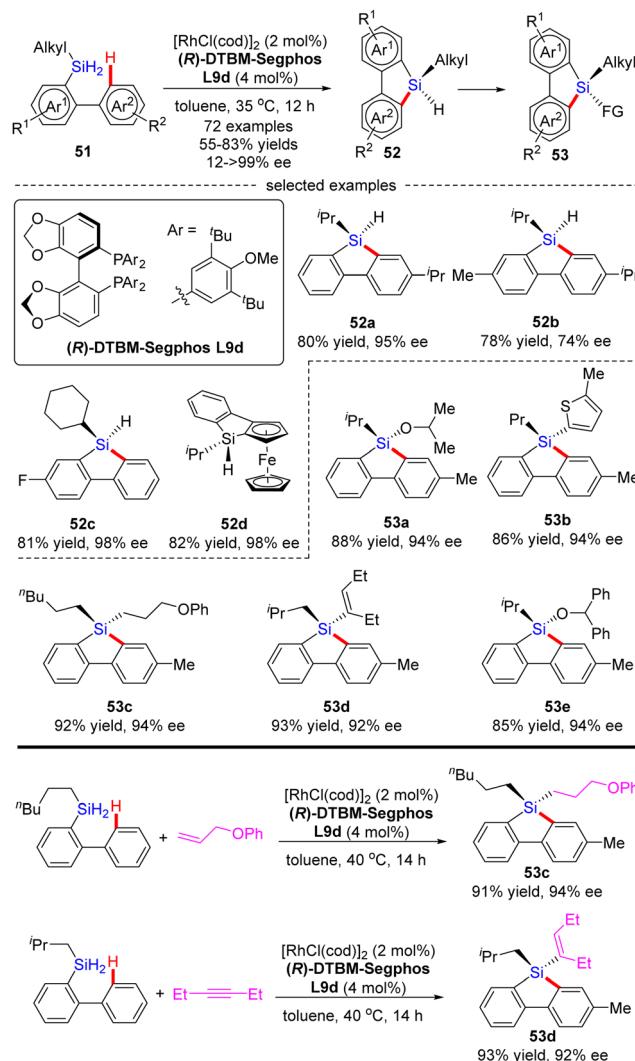
chiral benzosiloloferrocenes **50** as single diastereomers (dr > 20 : 1) with excellent enantioselectivities (90–99% ee). It is worth mentioning that several core scaffolds from pharmaceuticals, bioactive molecules, and materials, such as (–)-menthol,  $\beta$ -estradiol,  $\alpha$ -ribofuranoside, and pitavastatin fragment, were well accommodated in this reaction to furnish the corresponding benzosiloloferrocenes **50a–d** in 40–86% yields and 93–98% ee.

Most recently, He and co-workers described an elegant synthesis of chiral monohydrosilanes by Rh(i)-catalyzed intramolecular C-H silylation of dihydrosilanes (Scheme 16).<sup>85</sup> Under mild conditions, a diverse set of chiral monohydrosilanes **52** were obtained in 55–83% yields with favorable enantioselectivities (up to >99% ee). Substrates with substituents on both aryl rings were also compatible with this transformation, resulting in decreased yields and enantioselectivities (**52b**). Furthermore, a wide array of silicon-stereogenic and planar chiral ferrocene monohydrosilanes were successfully accessed by this approach with consistently excellent enantioselectivities (93–99% ee, *i.e.* **52d**). Unfortunately, only aryl alkyl





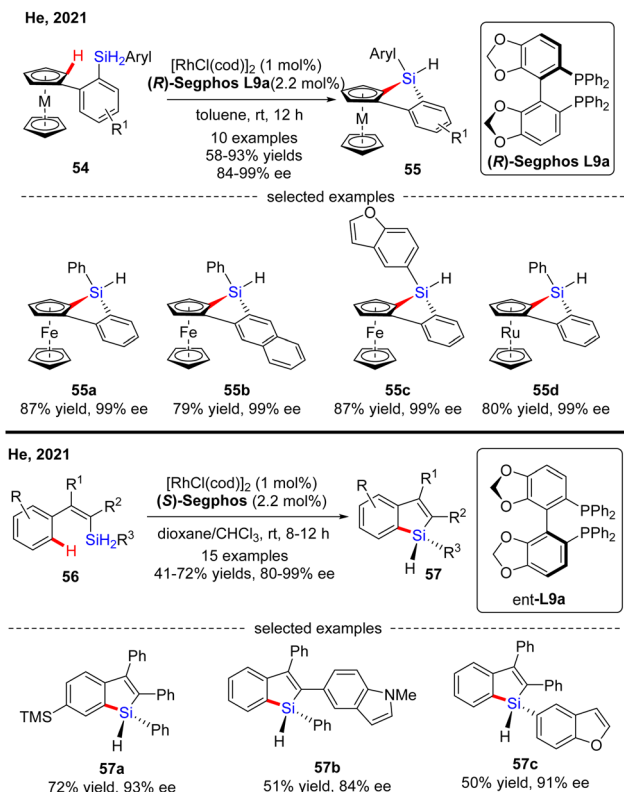
dihydrosilanes proved as competent substrates, whereas the use of diaryl dihydrosilanes was not successful in delivering the corresponding products, due to their decomposition issue in the presence of highly reactive rhodium catalysts. It is noteworthy that the resulting chiral monohydrosilanes 52 served as critical building blocks to effect the facile synthesis of different stereogenic tetraorganosilanes 53. While alcoholysis with isopropanol and C-H functionalization with 2-methylthiophene furnished products 53a and 53b, respectively, hydrosilylation with  $\pi$  bond compounds such as alkenes, alkynes, and ketones, delivered chiral tetraorganosilanes 53c-e via the construction of Si-C(sp<sup>2</sup>), Si-C(sp<sup>3</sup>), and Si-O bonds. In all cases, high yields were achieved with intact enantiocontrol. Remarkably, tandem C(sp<sup>2</sup>)-H silylation/hydrosilylation of dihydrosilanes with alkenes and alkynes also proved



**Scheme 16** Rh(i)-Catalyzed intramolecular C-H silylation of aryl alkyl dihydrosilanes.

successful, thus providing 53c and 53d in excellent yields and enantioselectivities.

Subsequently, He's group further expanded the substrate scope of the Rh(i)-catalyzed intramolecular C-H silylation reaction to diaryl dihydrosilanes (Scheme 17).<sup>86</sup> The key to the success of this transformation relied on decreased rhodium catalyst loading (1 mol%) to address the decomposition issue of the monohydrosilane products. To the authors' delight, a variety of silicon-stereogenic and planar chiral trisubstituted 1*H*-benzosiloloferrocenes 55 were achieved as single diastereomers with excellent enantioselectivities (84–99% ee). Furthermore, a ruthenocene-containing substrate was also compatible with this transformation, thus affording 55d in 80% yield and 99% ee. Meanwhile, with this catalytic system, He and co-workers effected asymmetric intramolecular dehydrogenative C-H silylation of alkenyl dihydrosilanes (Scheme 17).<sup>86</sup> With 1 mol% of rhodium catalyst, various alkenyl dihydrosilanes containing a diverse set of substituents at different positions were readily transformed into trisubstituted silicon-stereogenic 1*H*-

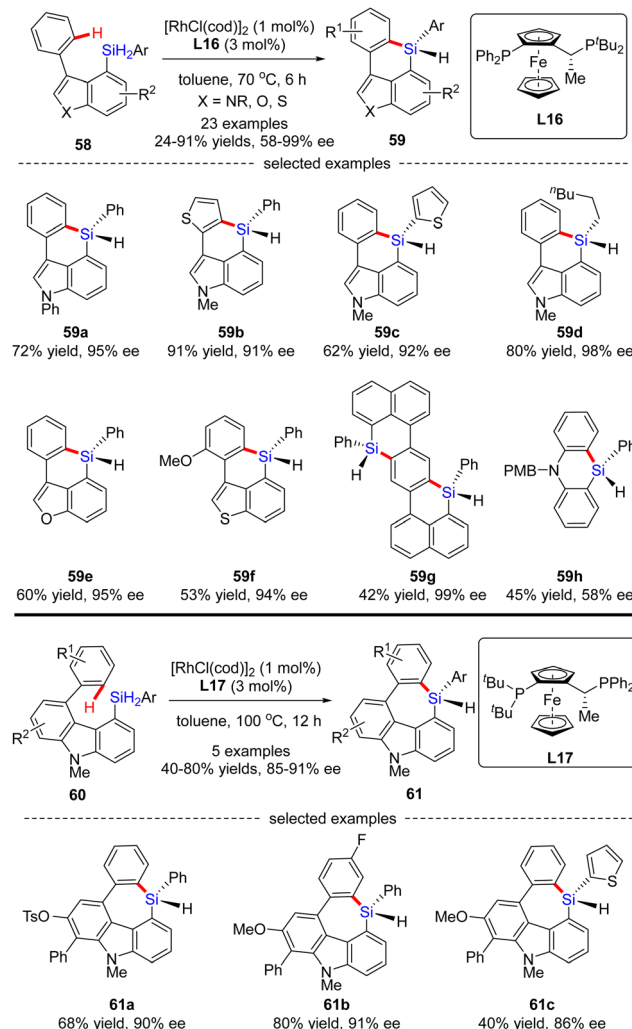


Scheme 17 Rh(i)-catalyzed intramolecular C–H silylation of diaryl and alkynyl dihydrosilanes.

benzosiloles 57 in moderate to decent yields (41–72%) and good to excellent enantioselectivities (80–99% ee).

Aside from a number of reports on the Rh(i)-catalyzed enantioselective construction of five-membered silicon-stereogenic silanes, most recently, He and co-workers disclosed a novel synthesis of six and seven-membered counterparts *via* asymmetric Rh(i) catalysis (Scheme 18).<sup>87</sup> Under the catalysis of [RhCl(cod)]<sub>2</sub> and Josiphos ligand L16, various silicon-bridged biaryls 58 consisting of benzene and indole moieties smoothly underwent dehydrogenative C–H silylation to provide a diverse set of six-membered silicon-stereogenic triorgano-substituted silanes 59 in 24–91% yields with excellent enantiocontrol (87–98% ee). It was found that high temperature was crucial to achieve high reactivity in this transformation. In addition to the indole scaffold, benzofuran, benzothiophene, and naphthalene counterparts were also well incorporated to afford silicon-stereogenic monohydrosilanes 59e–g in 94–99% ee. Furthermore, chiral silicon-bridged diphenylamine 59h could also be accessed by this approach, despite a much lower enantioselectivity (58% ee). It is noteworthy that several seven-membered carbazole-based silicon-stereogenic triorgano-substituted silanes 61 were readily obtained in moderate to good yields (40–80%) and decent enantioselectivities (85–91% ee) by simply replacing the chiral ligand L16 with L17.

Subsequently, He and co-workers disclosed a cascade desymmetric Si–C activation/C–H silylation and intermolecular dehydrogenative silylation reaction of silacyclobutanes (SCB) 62

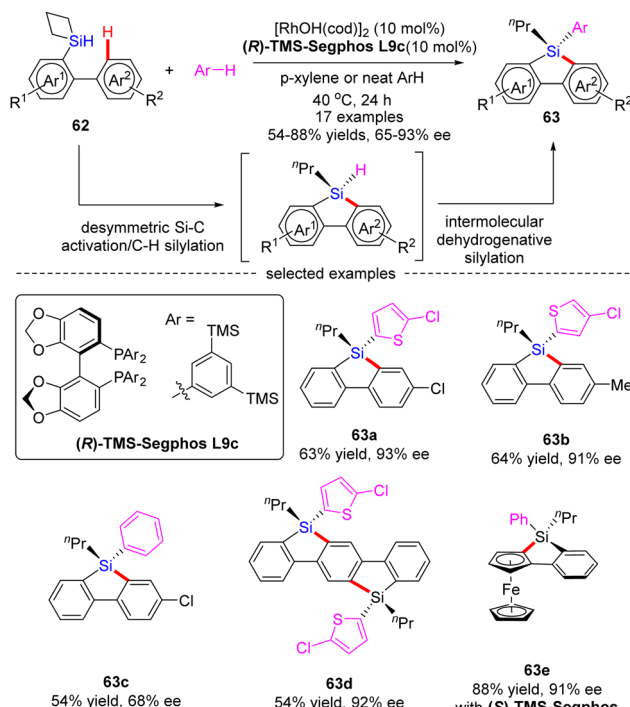


Scheme 18 Rh(i)-Catalyzed synthesis of six- and seven-membered silicon-stereogenic triorgano-substituted silanes.

with arenes *via* asymmetric Rh(i) catalysis (Scheme 19).<sup>88</sup> As a result, a variety of quaternarily silicon-stereogenic dibenzosiloles 63 were attained in moderate to high yields (54–88%) and good enantioselectivities (65–93% ee). Aside from thiophene derivatives, benzene also proved as capable substrate to furnish the corresponding silole 63c in comparable yield, but diminished enantiocontrol (68% ee). Notably, by taking advantage of this catalytic system, bis-silole 63d and ferrocene silole 63e were achieved in 92% ee and 91% ee, respectively.

Most recently, the Rh(i)-Catalyzed intermolecular asymmetric C–H silylation was independently successfully realized by W. He and C. He (Scheme 20).<sup>89</sup> As described by W. He and co-workers, with biphenylphosphine L11b as a chiral ligand, various silacyclobutanes 64 were smoothly coupled with thiophene derivatives 65, forging chiral acyclic monohydrosilanes 66 in moderate to excellent yields (50–82%) and stereo-control (54–96% ee). The reaction was proposed to commence with the generation of intermediate Int-18 *via* thiophene coordination to the pre-formed [Rh]–H catalyst. Subsequent oxidative addition of silacyclobutane 64 onto Rh(i) in Int-18 proceeded to afford a



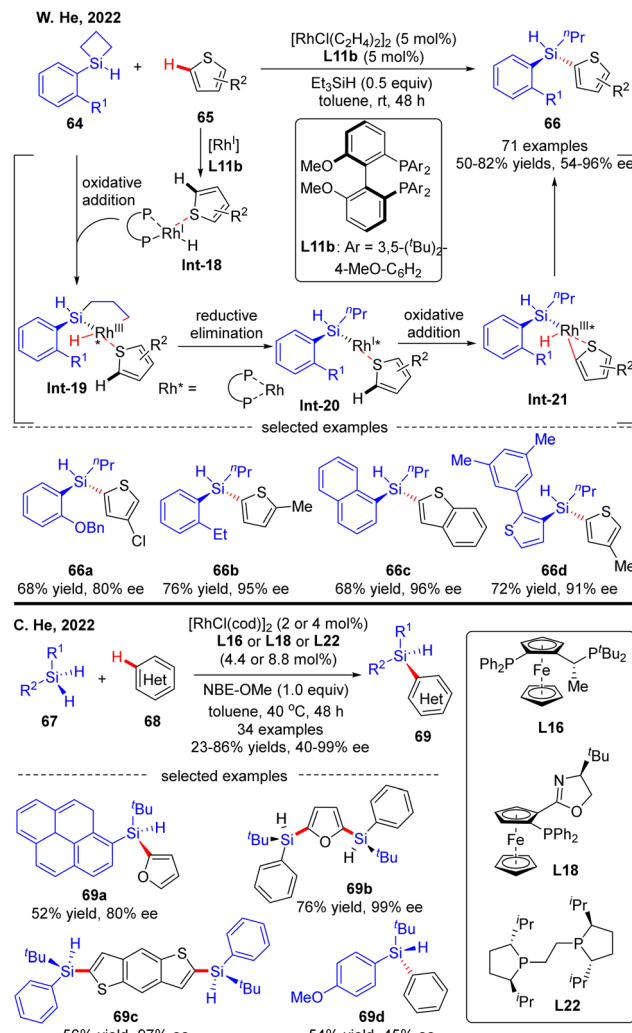


**Scheme 19** Rh(I)-Catalyzed asymmetric desymmetrization/C-H silylation/dehydrogenative silylation of silacyclobutanes.

five-membered rhodacycle **Int-19**. Reductive elimination of rhodacycle **Int-19** occurred to form **Int-20**, which then underwent C-H activation to furnish oxidative addition intermediate **Int-21**. Finally, the desired acyclic stereogenic monohydrosilane **66** was obtained *via* a second reductive elimination of **Int-21**. Almost at the same time, C. He and co-workers also communicated a Rh(I)-catalyzed intermolecular asymmetric C-H silylation of heteroarenes *via* a direct dehydrogenative C-H/Si-H cross-coupling (Scheme 20).<sup>90</sup> As a result, a diversity of acyclic heteroarylated silicon-stereogenic monohydrosilanes **69** including bis-Si-stereogenic silanes (**69b**, **69c**) were generated in decent yields and enantioselectivities. Notably, apart from furan and thiophene derivatives, simple arenes were also compatible with this reaction, despite moderate stereo-control (**69d**). It was worth mentioning that the use of norbornene derivative NBE-OMe as a hydrogen acceptor was critical to maintaining the reactivity.

## 2.2 Functionalization of C(sp<sup>3</sup>)-H bonds

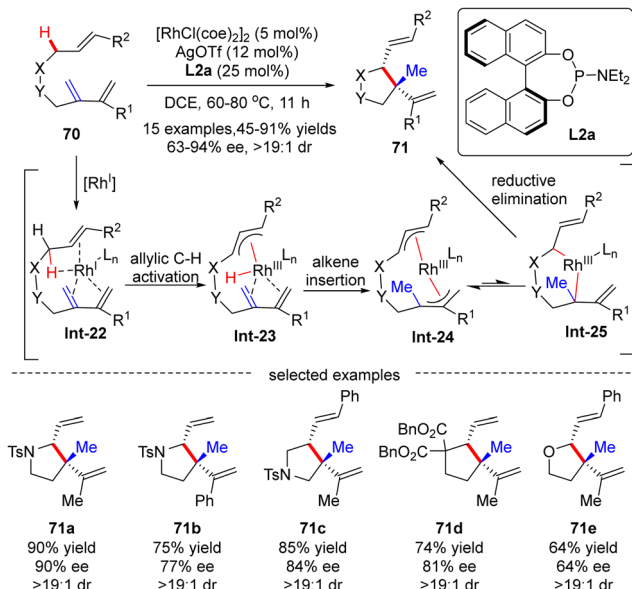
**2.2.1 Functionalization of activated C(sp<sup>3</sup>)-H bonds.** In 2012, Yu's group reported a Rh(I)-catalyzed asymmetric functionalization of activated allylic C(sp<sup>3</sup>)-H bonds for intramolecular addition to conjugated 1,3-dienes.<sup>91</sup> Various nitro-tethered ene-2-dienes **70** containing either alkyl or aryl substituents were readily converted to pyrrolidine derivatives **71** in 45–91% yields with moderate to excellent enantioselectivities (63–94% ee), using [RhCl(cod)<sub>2</sub>] as a catalyst, AgOTf as a co-catalyst and (S)-binaphthol (BINOL)-derived monodentate phosphoramidite **L2a** as a chiral ligand. Moreover, carbon- and oxygen-tethered ene-2-dienes were also suited to this



**Scheme 20** Rh(I)-Catalyzed intermolecular asymmetric C-H silylation.

transformation, providing cyclopentane and tetrahydrofuran derivatives **70d** and **70e** in 81% and 64% ee, respectively. Notably, two adjacent stereo-centers with one quaternary carbon center were constructed in excellent diastereoselectivities (dr > 19:1). The underlying mechanism was next thoroughly investigated based on the DFT (density functional theory) calculation (Scheme 21).<sup>92</sup> As depicted in Scheme 21, the reaction was initiated by the coordination of the rhodium catalyst with the substrate, leading to the formation of Rh-complex **Int-22**. Follow-up allylic C-H activation provided rhodium-hydride species **Int-23**, which then underwent alkene insertion to furnish bis-allylic Rh-complex **Int-24**. Finally, di- $\pi$ -allyl-assisted reductive elimination of **Int-25** occurred to release the desired product.

In 2016, Glorius's group reported a Rh(I)-catalyzed asymmetric approach for the site- and *enantio*-selective intermolecular arylation of benzylic C(sp<sup>3</sup>)-H bonds (Scheme 22).<sup>93</sup> Diverse triarylmethanes **74** were achieved in 42–86% yields and with moderate to good enantioselectivities (62–80% ee) by reacting 8-benzyl quinolones **72** with aryl bromides **73** under the catalysis of RhCl(PPh<sub>3</sub>)<sub>2</sub> and NHC (*N*-heterocyclic carbene)

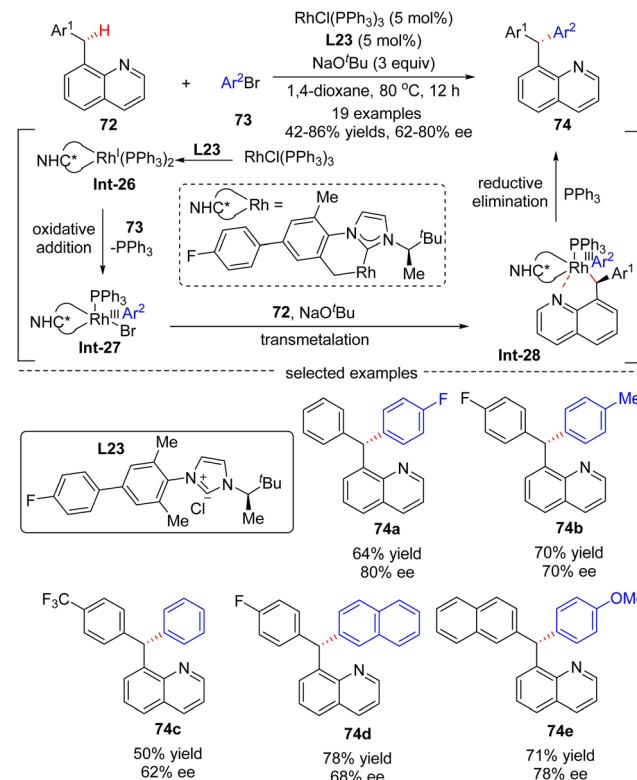


Scheme 21 Rh(I)-Catalyzed allylic C–H activation and addition to conjugated dienes.

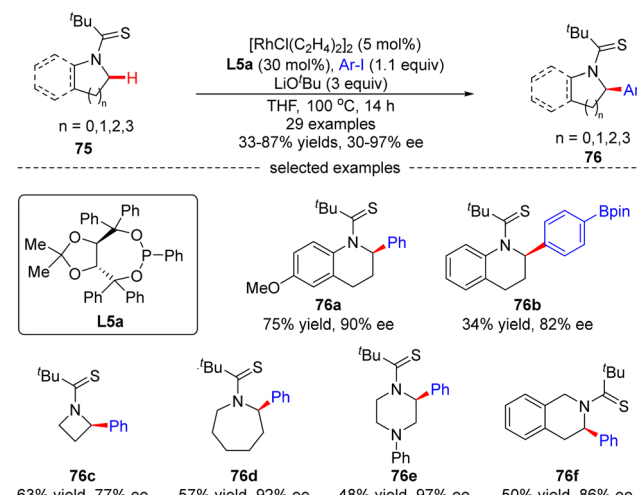
pre-ligand **L23**. The underlying plausible reaction mechanism was proposed as depicted in Scheme 22. First, reactive intermediate Rh(I)-complex **Int-26** was generated by the coordination of *in situ* generated free NHC to rhodium, followed by intramolecular activation of a benzylic C–H bond on the carbene ligand. Then, Rh(III) species **Int-27** was formed by oxidative addition of aryl bromides into **Int-26**, with concomitant elimination of associated ligand  $\text{PPh}_3$ . Afterwards, Rh-complex **Int-28** was produced by a *trans*-metalation reaction of **Int-27** with deprotonated substrate **72**, which was generated by an excess amount of  $\text{NaO}^\text{t} \text{Bu}$ . Finally, the desired product **74** was achieved *via* reductive elimination of **Int-28**.

Glorius's group later explored another Rh(I)-catalyzed approach for the enantioselective intermolecular C( $\text{sp}^3$ )-H arylation of tetrahydroquinolines and other saturated N-heterocycles with aryl iodides, without observation of the arylation of the adjacent C( $\text{sp}^2$ )-H bonds on tetrahydroquinolines (Scheme 23).<sup>94</sup> In this reaction, the combination of  $[\text{RhCl}(\text{C}_2\text{H}_4)]_2$  and chiral phosphonite ligand **L5a** acted as a powerful catalytic system producing a diversity of  $\alpha$ -arylated N-heterocycles with high regio- and *enantio*-selectivity, while using *tert*-butyl thioamide as a directing group. Both electron-donating and electron-withdrawing substituents on the phenyl ring were well tolerated when the tetrahydroquinoline scope was concerned. Substituents such as cyano, thioanisoles, trifluoromethyl, and arylboronic pinacol esters were also compatible in the case of aryl iodides. Remarkably, the scope of saturated aza-heterocycles could be extended to piperidine, pyrrolidine, piperazine, azepane and azetidine, and the corresponding  $\alpha$ -N-arylated products **76c–f** were obtained in good regio- and *enantio*-selectivities (up to 97% ee).

**2.2.2 Functionalization of unactivated C( $\text{sp}^3$ )-H bonds.** In 2015, Takai's group shared their pioneering work on the enantioselective rhodium-catalyzed dehydrogenative silylation



Scheme 22 Rh(I)-Catalyzed intermolecular C–H arylation of 8-benzyl quinolones and aryl bromides.

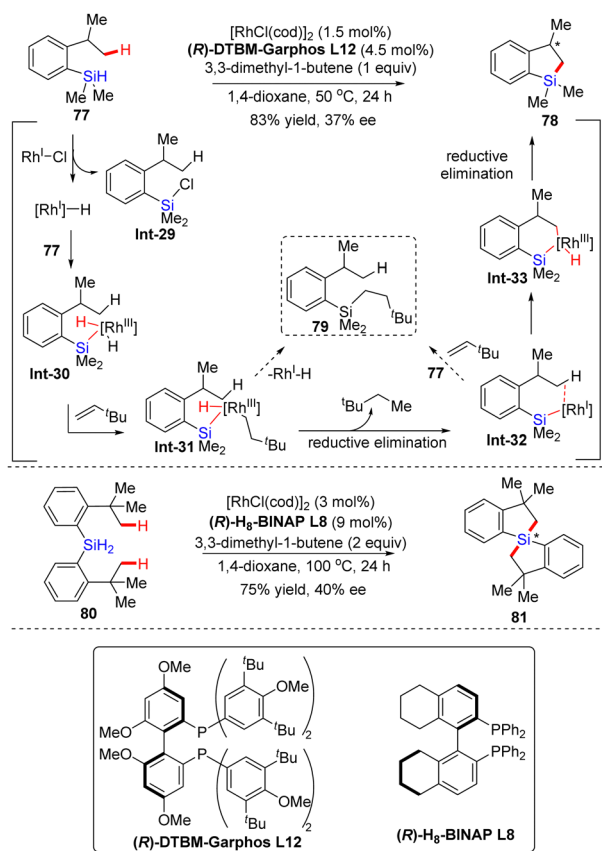


Scheme 23 Rh(I)-Catalyzed intermolecular C–H arylation of tetrahydroquinolines and saturated aza-heterocycles.

of unactivated C( $\text{sp}^3$ )-H bonds (Scheme 24).<sup>95</sup> In the presence of  $[\text{RhCl}(\text{cod})]_2$ ,  $C_2$ -symmetric diphosphine ligand (*R*)-DTBM-Garphos **L12** and hydrogen acceptor 3,3-dimethyl-1-butene, 2-isopropylphenylsilane **77** was converted to 2,3-dihydrobenzo[b]silole **78** in 83% yield without any formation of hydroxylated product **79**, in spite of the low enantiocontrol (37% ee) (Scheme 24). While ligand (*R*)-DTBM-Garphos was replaced



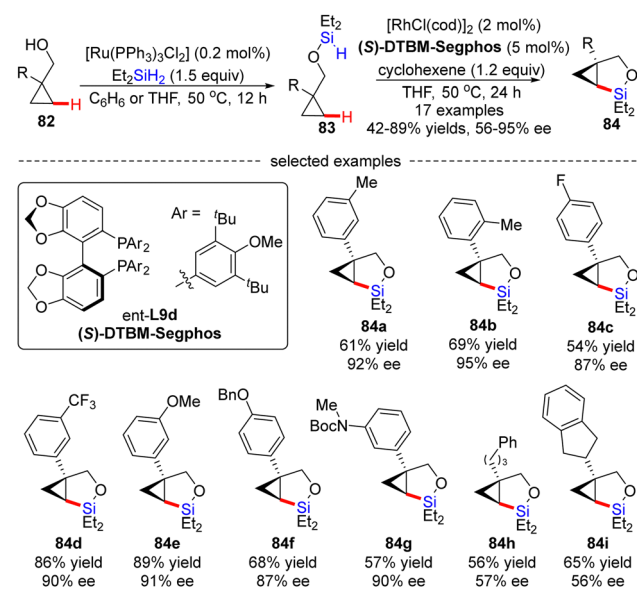
with *(R)*-H<sub>8</sub>-BINAP **L8**, 1,1'-spirosilabiindane **81** with a new tetrasubstituted silicon-stereogenic center was achieved in comparable yield (75%) and enantioselectivity (40% ee) *via* dual asymmetric alkylation of dihydrosilane **80** at elevated temperature with increased catalyst and hydrogen acceptor loading. The mechanism of this unique reaction has also been proposed as given in Scheme 24. First, hydrosilane **77** was oxidatively added to the Rh(i)-Cl pre-catalyst, furnishing a Rh(i)-H species involving the reductive elimination of chlorosilane **Int-29**. The Rh(i)-H species was then added to the Si-H bond of **77**, and the resulting intermediate **Int-30** further reacted with 3,3-dimethyl-1-butene to produce intermediate **Int-31**. Instead of the hydrosilylated product **79**, Rh-silyl species **Int-32** was preferably formed by reductive elimination of H and 3,3-dimethylbutane groups on the rhodium center of **Int-31**, which might be attributed to the tendency of 3,3-dimethylbutyl and sterically bulky silyl groups to keep distance from each other. The hydrosilylated product **79** might be generated by the reaction of **Int-32** with 3,3-dimethyl-1-butene *via* silylrhodation followed by the Sigma-bond metathesis with **77**. However, the electron-rich Rh center in **Int-32** favored intramolecular oxidative addition over the silylrhodation to provide **Int-33**, which then underwent reductive elimination to generate the desired product **78**.



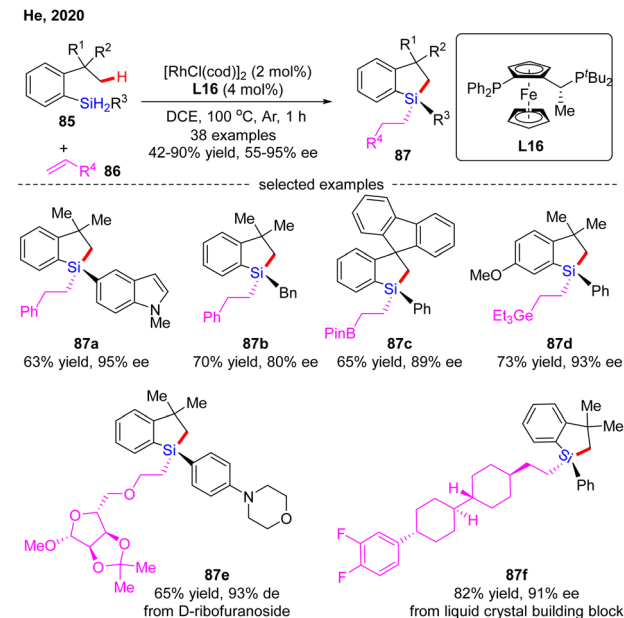
Scheme 24 Rh(i)-Catalyzed intramolecular C-H silylation of 2-isopropylphenylsilane and dihydrosilane.

Soon after, Hartwig's group described an unprecedented enantioselective intramolecular silylation of cyclopropyl C-H bonds in the presence of a Rh catalyst.<sup>96</sup> As displayed in Scheme 25, silyl ether **83** was *in situ* generated by Ru-catalyzed dehydrogenative coupling of cyclopropylmethanols **82** with diethylsilane and was used in the follow-up reaction without further purification. In the presence of [RhCl(cod)]<sub>2</sub>/(S)-DTBM-Segphos and a hydrogen acceptor cyclohexene, the intramolecular silylation of silyl ethers **83** readily occurred to generate various bicyclic silylcyclopropanes **84** in decent to high yields (42–89%) with moderate to good enantiomeric excesses (56–95% ee). Generally, aryl-substituted cyclopropylmethanols provided higher enantioselectivities compared with alkyl-substituted substrates (**84a–g** *vs.* **84h–i**), which was contributed by an additional  $\pi$ - $\pi$  interaction between the aryl moieties of the substrate and the Rh(i) catalyst. Mechanistic studies suggested that the C-H cleavage might be the turnover-limiting step and determined the configuration of the product.

In 2020, He and co-workers developed a Rh(i)-catalyzed enantioselective silylation of unactivated C(sp<sup>3</sup>)-H bonds, thus providing an elegant access to silicon-stereogenic dihydrosiloles (Scheme 26).<sup>97</sup> This reaction comprises a two-step sequence, namely a highly asymmetric silylation of C(sp<sup>3</sup>)-H bonds in dihydrosilanes and a follow-up stereospecific alkene hydrosilylation. With *(R,Sp)*-Josiphos **L16** as a chiral ligand, a diverse set of dihydrosilanes **85** and alkenes **86** were well compatible with this reaction to afford various silicon-stereogenic tetrasubstituted silanes **87** in good to excellent yields (42–90%) and enantioselectivities (55–95% ee). Shortly after, He and co-workers further disclosed an elegant approach to axially chiral 6-member-bridged biaryl derived dihydrosiloles with a silicon-stereogenic center *via* Rh(i)/**L16** catalysis.<sup>98</sup> A diverse set of silicon-centrally and axially dihydrosiloles **89** were conveniently generated in 35–78%



Scheme 25 Rh(i)-Catalyzed intramolecular C-H silylation of hydrosilyl ethers.



Scheme 26 Rh(I)-Catalyzed asymmetric silylation of unactivated  $C(sp^3)$ -H bonds.

yields and 83–96% ee. It was found that the presence of a hydrogen acceptor such as a norbornene derivative (NBE-OMe) was crucial to enhance the reactivity.

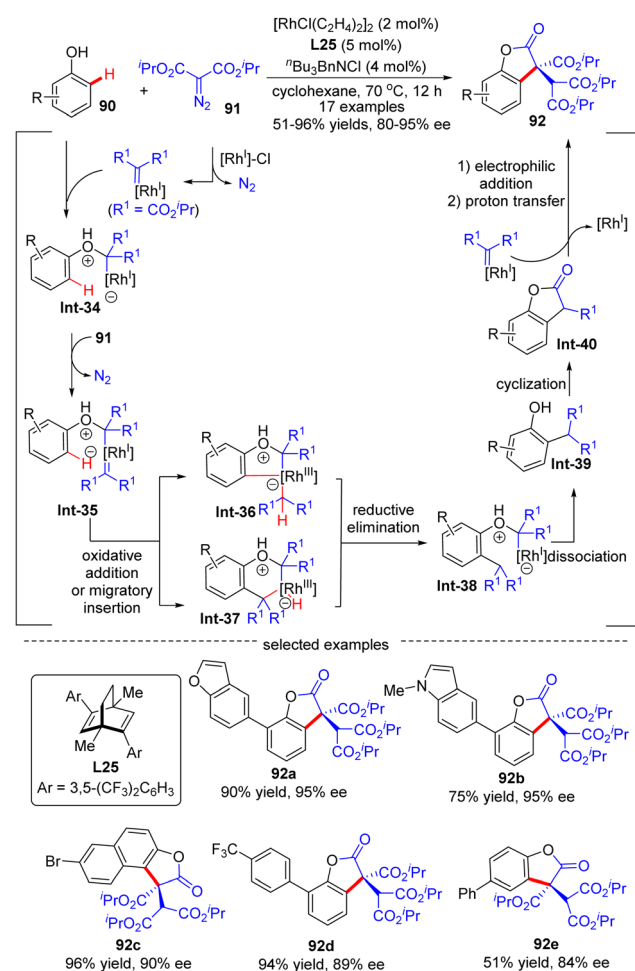
### 3. Outer-sphere C–H functionalization

The outer-sphere mechanism does not involve the direct interaction of the metal with the C–H bond, but instead commences with the formation of a rhodium-carbenoid, -nitrenoid, or -oxo species, followed by the reaction of this species with the C–H bond *via* either a direct insertion or a hydrogen atom transfer (HAT)/radical rebound pathway.

In 2020, Wang's group demonstrated an example of carbene *ortho*-selective  $C(sp^2)$ -H insertion of phenols with diisopropyl diazomalonate *via* Rh(I)/diene catalysis (Scheme 27).<sup>99</sup> With a transient oxonium ylide as the directing group, the final tris-carboxylate-substituted 2-benzofuranones 92 bearing a quaternary all-carbon center were produced in good yields (51–96%) and enantioselectivities (80–95% ee). The substrate scope investigation showed that various substituents at the *ortho*,

*meta*- and *para*-position were all well tolerated, indicating the good functional-group tolerance of this reaction. The underlying mechanism was proposed as shown in Scheme 27. Generally, this reaction was initiated by Rh(I)-triggered  $N_2$  extrusion from 91 to form a Rh-carbene intermediate, which then reacted with phenol to give an oxonium ylide Int-34. Int-34 promoted the extrusion of  $N_2$  from a second 91, giving access to another Rh-carbene species Int-35. Subsequently, Int-35 underwent *ortho*-C( $sp^2$ )-H oxidative addition/migratory insertion sequence to produce Int-36 or Int-37, which then experienced a reductive elimination to provide Int-38. Afterwards, Int-40 was formed by dissociation of the oxonium ylide Int-38 and follow-up cyclization of Int-39. Finally, Int-40 proceeded with electrophilic addition to another Rh-carbene, followed by proton transfer to release the desired product 92.

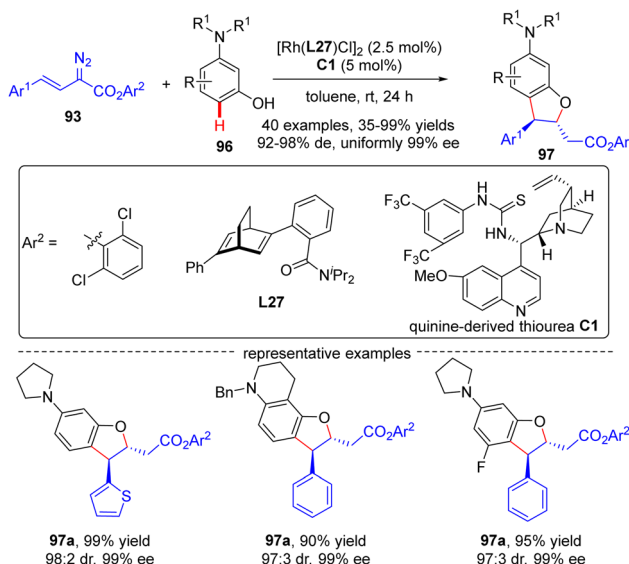
In 2021, Xu and co-workers developed an elegant Rh(I)/diene-catalyzed regiospecific and enantioselective arylvinylcarbene insertion of the  $C(sp^2)$ -H bond of aniline derivatives (Scheme 28).<sup>100</sup> The reaction was characterized by multiple merits, such as unusual regio-selectivity at the vinyl terminus site, excellent *E*-selectivity and enantioselectivities (82–95% ee), simple and mild conditions, and broad functional group



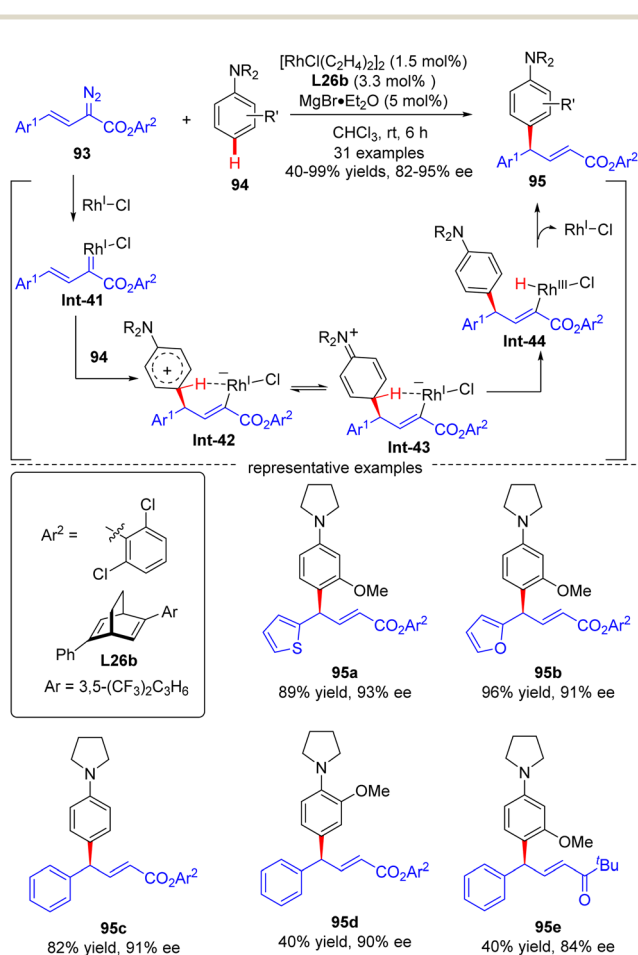
Scheme 27 Rh(I)-Catalyzed enantioselective  $C(sp^2)$ -H functionalization of phenols with diisopropyl diazomalonate.



tolerance, offering access to a diversity of chiral  $\gamma,\gamma$ -*gem*-diarylsubstituted  $\alpha,\beta$ -unsaturated esters **95**. Synthesis applications of this protocol were featured by several versatile product transformations. Apart from arylvinyl diazoacetates, a more challenging arylvinyl diazoketone substrate was also found to be compatible with this transformation, giving rise to the expected C–H functionalization product **95e** in moderate yield (40%) and good enantioselectivity (84% ee). Combined experimental and computational studies were carried out to elucidate the reaction mechanism. Initially, arylvinyl diazoacetate reacted with the active monorhodium catalyst Rh–Cl to afford the Rh(i)-arylvinylicarbenoid intermediate **Int-41**. The ensuing addition of the electron-rich phenyl ring of aniline onto **Int-41** site-selectively occurred at the vinyl terminus site to furnish zwitterionic species **Int-42**, which then proceeded a 1,5-proton transfer event to provide Rh(III) species **Int-44**. Finally, reductive elimination of **Int-44** happened, leading to the desired product **95** and the regeneration of the monorhodium catalyst. Of note, an inverse deuterium kinetic isotope effect was observed in this reaction, supporting the C–C bond-formation step as a rate-determining step. Encouraged by this elegant work, Xu and co-workers further realized a one-pot rhodium-catalyzed C–H functionalization/organocatalyzed oxa-Michael addition cascade reaction



Scheme 29 Rh(i)-Catalyzed enantioselective C–H functionalization/oxa-Michael addition cascade.

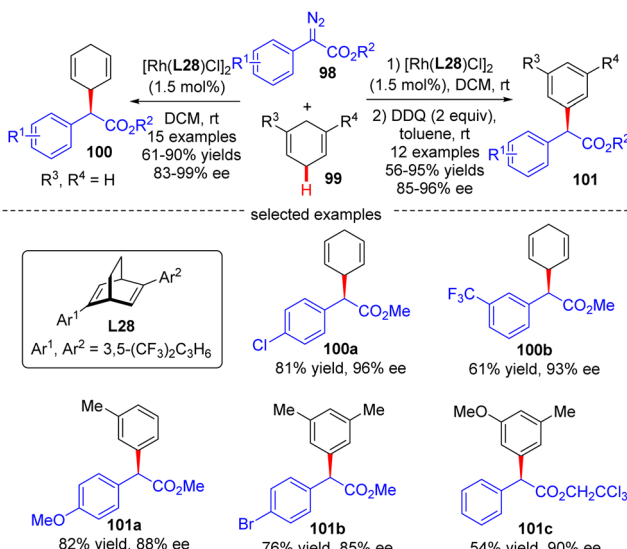


Scheme 28 Rh(i)-Catalyzed enantioselective arylvinylcarbene insertion of the C–H Bond of aniline derivatives.

of 3-hydroxyaniline derivatives **96** with arylvinyl diazoacetate **93** (Scheme 29).<sup>101</sup> Under mild conditions, a diverse set of 2,3-disubstituted dihydrobenzofurans **97** were attained in good yields (up to 99%) and excellent stereoselectivity (92–98% de, uniformly 99% ee). It was noteworthy that the two contiguous stereogenic centers of product **97** were independently controlled by two chiral catalysts *via* a one-pot two-step operation. As a consequence, the full complement of stereoisomers could be accessed at will by appropriate permutations of the two chiral catalysts.

In 2021, Xu's group developed an asymmetric Rh(i)/diene-catalyzed C(sp<sup>3</sup>)–H functionalization of 1,4-cyclohexadiene **99** with  $\alpha$ -aryl-diazoacetate **98**, which provided a direct access to various chiral 2-arylacetates **100** in good yields (up to 90%) and enantiomeric excess (up to 99%) (Scheme 30).<sup>102</sup> The application of this reaction was further highlighted by the follow-up oxidation of the products with DDQ with the generation of diverse enantioenriched  $\alpha,\alpha$ -diarylacetates **101**. Notably, the steric factor had a great impact on the reactivity of different C(sp<sup>2</sup>)–H bonds, and only the less sterically hindered C(sp<sup>2</sup>)–H bonds were functionalized.

In 2022, Xu and co-workers communicated an elegant Rh(i)-diene catalyzed highly enantioselective C(sp<sup>2</sup>)–H allylation of simple unprotected indoles, pyrroles, and their common analogues such as furans, thiophenes, and benzofurans with arylvinyl diazoesters, offering a facile and reliable access to a diversity of diarylmethane-containing  $\alpha,\beta$ -unsaturated esters **104** & **106** in favorable yields (73–99%), and excellent enantioselectivities (70–97% ee) (Scheme 31).<sup>103</sup> For unprotected indole substrates **103** without a substituent at the C3 position, the carbene insertion site selectively occurred at the C3 position of indoles. In contrast, when unprotected pyrroles were used or the C3 position of indoles, furans, thiophenes and benzofurans (**105**) were occupied by a protected amino group, only C2 carbene insertion proceeded. Notably, the bulky 2,4,6-



Scheme 30 Rh(i)-Catalyzed enantioselective  $C(sp^3)$ -H functionalization of 1,4-cyclohexadiene with  $\alpha$ -aryl-diazoacetates.

trimethylphenyl substituent on arylvinyl diazoesters was found to be critical to guarantee the excellent enantioselectivity of this reaction and this reaction was also characterized by an uncommon site-selectivity at the vinyl terminus of arylvinylcarbene. Mechanistic experiments and DFT calculations indicated that the C–C addition barrier was lowered by the more electron-rich indole substrate, thus changing the rate-determining step to the reductive elimination step. Soon after, Xu and co-workers further extended the substrate scope of Rh(i)-diene catalysed arylvinylcarbene insertion process to *N*-protected indoles **107**, giving rise to an interesting class of chiral indole scaffolds **108** containing a *gem*-diaryl carbon stereocenter in good yields (up to 99%) and excellent enantioselectivities (up to 96% ee).<sup>104</sup>

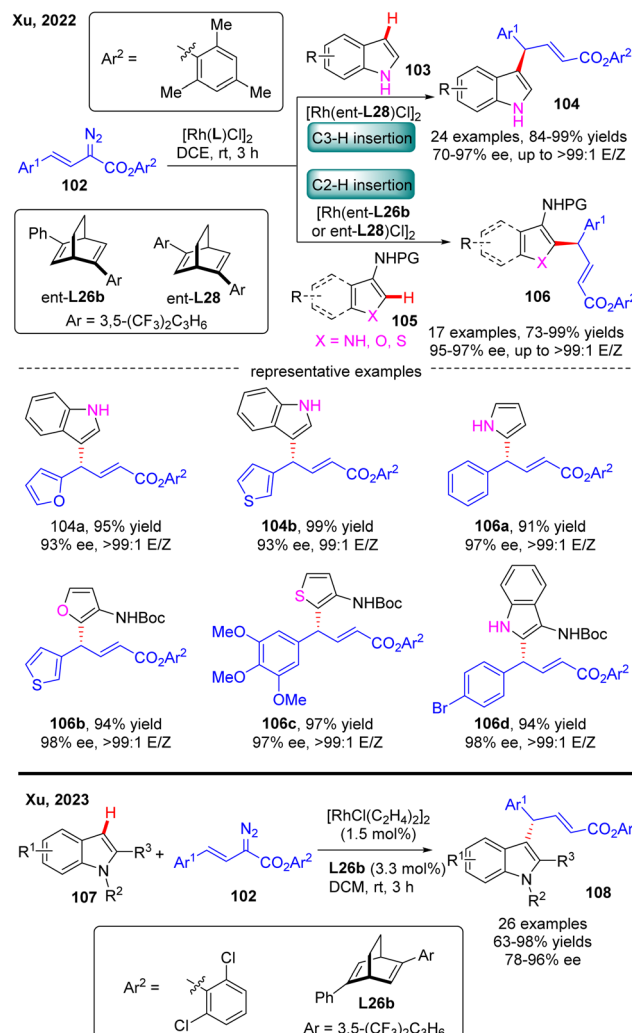
## 4. C–H functionalization *via* 1,4-Rh migration

Aside from the above-described Rh(i)-catalyzed direct C–H activation *via* either an inner- or outer-sphere mechanism, 1,4-Rh migration represents an alternative approach to promote C–H activation to form unique carbon–Rh bonds, which could be further transformed into a diversity of valuable scaffolds. More importantly, 1,4-Rh migration could facilely introduce a rhodium moiety into a specific position of an organic molecular skeleton, which would be otherwise difficult to be obtained *via* classic approaches. Currently, the most prevalent 1,4-Rh migration for asymmetric C–H functionalization is from alkenyl to aryl, despite that several other modes such as alkyl-to-aryl, aryl-to-alkenyl, allyl-to-allyl, and alkenyl-to-allyl 1,4-Rh migration may also exist.

### 4.1. $C(sp^2)$ -H functionalization *via* 1,4-Rh migration

#### 4.1.1 $C(sp^2)$ -H functionalization *via* alkenyl-to-aryl 1,4-Rh migration.

In 2006, Hayashi's research group developed an



Scheme 31 Rh(i)-Catalyzed enantioselective  $C(sp^2)$ -H functionalization of simple unprotected indoles, pyrroles and heteroanalogues and protected indoles.

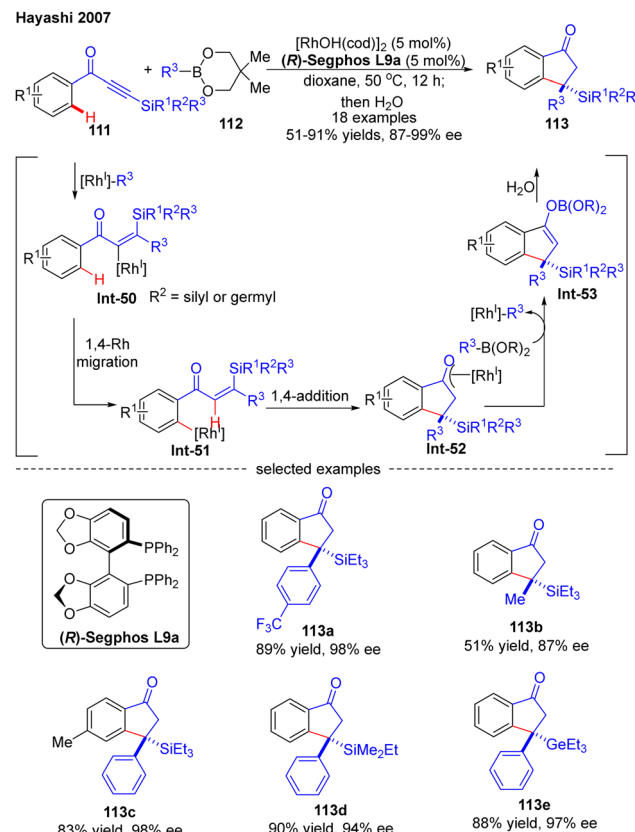
effective Rh(i)-catalyzed asymmetric synthesis of 3-substituted 1-indanones *via* an alkenyl-to-aryl 1,4-Rh migration (Scheme 32).<sup>105</sup> By employing a newly designed axially chiral bisphosphine ligand **L14**, wherein the absolute configuration of the 3-3' axis was fixed to (*R*) after complexation to transition metal rhodium, they successfully prepared several indanones **110** in 44–60% yields with 92–99% ee *via* an asymmetric isomerization of racemic  $\alpha$ -arylpolypropyl alcohols **109**. The underlying mechanism was studied, suggesting that this reaction was initiated by the ligand exchange of **109** by Rh(i) catalyst to generate alkoxyrhodium **Int-45**. Subsequent  $\beta$ -H elimination of **Int-45** followed by conjugate hydrorhodation resulted in alkenylrhodium species **Int-47**, which further underwent 1,4-rhodium migration to provide **Int-48**. Afterwards, **Int-49** with a new emerging stereocenter was produced by intramolecular 1,4-addition of **Int-48**. The Rh(*R,R*)-**L13** complex played an important role in this step, as it could recognize the enantio-topic face of the C–C double bond in **Int-48** to create a new



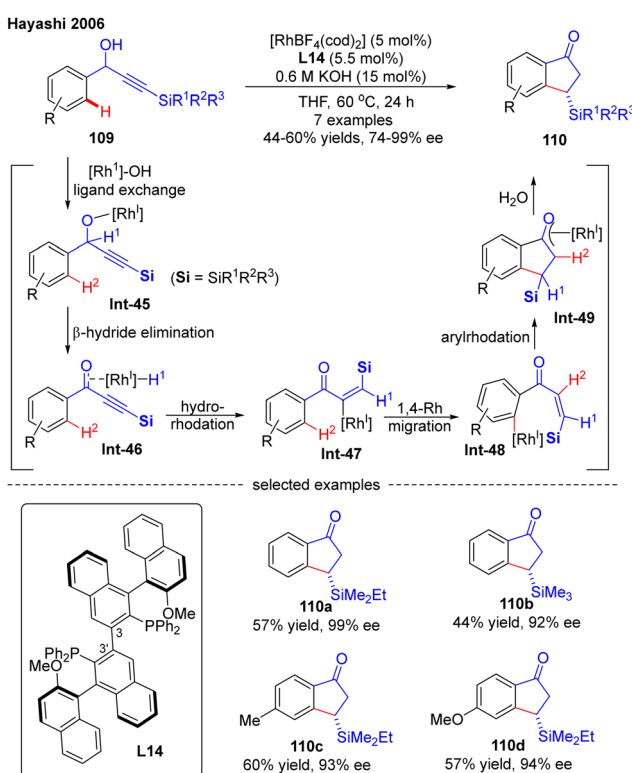
stereocenter with high enantioselectivity. The desired product **110** was finally obtained by the hydrolysis of **Int-49**.

In 2007, Hayashi and co-workers further reported a  $[\text{RhOH}(\text{cod})_2]/(\text{R})\text{-Segphos}$  catalytic system for high enantioselective addition of boronates **112** to aryl silyl ethynyl ketones **111** (Scheme 33).<sup>106</sup> With this system, a variety of 3,3-disubstituted 1-indanones **113** were obtained in impressive yields (51–91%) and excellent enantiomeric excess (87–99%). Aside from the silyl substituents on the ethynyl ketones, a germyl substituted substrate was also compatible with this reaction to give the corresponding product **113e** in 88% yield and 97% ee. The underlying mechanism of the reaction was also proposed (Scheme 33). First, insertion of the alkyne group in **111** into the  $[\text{Rh}]$ -carbon bond generated the alkenyl rhodium species **Int-50**, which underwent a 1,4-Rh migration process to produce the aryl rhodium intermediate **Int-51**. Subsequent 1,4-intramolecular addition in **Int-51** occurred to deliver the oxa- $\pi$ -allyl rhodium species **Int-52**, wherein the stereochemistry was determined. Follow-up transmetalation of **Int-52** with boronates **112** released the boron enolate **Int-53** along with the  $[\text{Rh}]$ - $\text{R}^3$  species for the next cycle. Finally, the desired product **113** was achieved by hydrolysis of **Int-53**.

The asymmetric synthesis of enantiopure spirocyclics, a class of prevalent scaffolds in natural products, biologically active molecules and chiral ligands, has gained great attention in organic chemistry. In 2010, Hayashi's group communicated a facile access to chiral spirocyclics *via* a Rh(i)/diene catalyzed enantioselective addition of sodium tetraarylborates



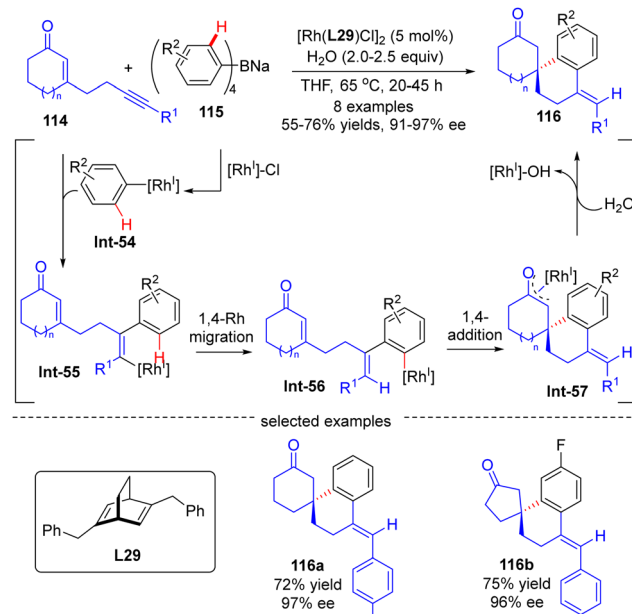
Scheme 33 Rh(i)-Catalyzed enantioselective addition of aryl boronates to aryl alkynyl ketones.



Scheme 32 Rh(i)-Catalyzed enantioselective isomerization of racemic  $\alpha$ -arylpropargyl alcohols.

**115** to alkyne-tethered 2-cycloalken-1-ones **114** (Scheme 34).<sup>107</sup> With sodium tetraarylborates **115** as surrogates of 1,2-dimetalloarenes and the chiral diene **L28** as a ligand, a variety of spirocycles **116** bearing a quaternary carbon stereocenter were prepared in good yields (55–76%) and a decent enantioselective excess (91–97%). This reaction was proposed to be initiated by the generation of an aryl-Rh species **Int-54** *via* the transmetalation of **115** with  $[\text{Rh}]\text{-Cl}$ . **Int-54** underwent insertion of the alkyne group in **114** to generate alkenyl-Rh intermediate **Int-55**, which was then converted to aryl-Rh species **Int-56** *via* a 1,4-Rh migration process. Successive intramolecular 1,4-addition onto the tethered enone moiety in **Int-56** resulted in oxa- $\pi$ -allyl-Rh intermediate **Int-57**. The final hydrolysis of **Int-57** released the desired product **116** along with concurrent regeneration of the Rh(i) catalyst.

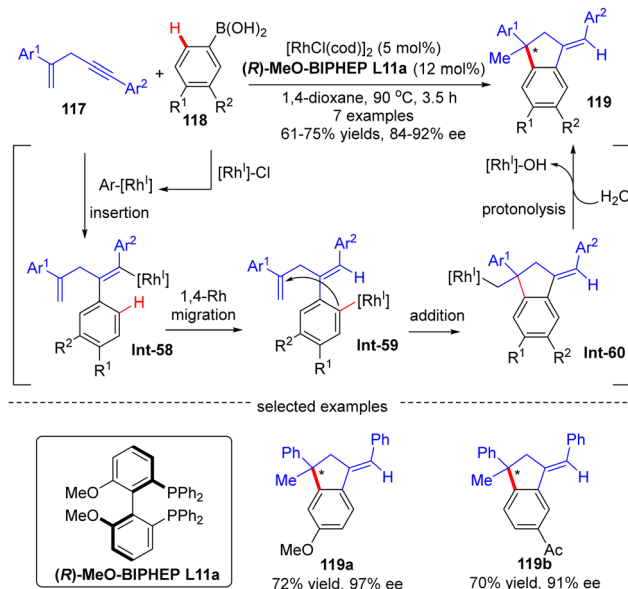
Afterwards, Matsuda and co-workers reported the asymmetric synthesis of indanes **119** possessing a quaternary all-carbon center from 1,4-enynes **117** with arylboronic acids **118** *via* a Rh(i)-catalyzed arylation/annulation process (Scheme 35).<sup>108</sup> The desired indanes **119** were readily obtained with yields of 61–75% and enantiomeric excess of 84–92% by taking advantage of the  $[\text{Rh}(\text{cod})\text{OH}]_2/(\text{R})\text{-MeO-BIPHEP}$  catalytic system. As far as this reaction mechanism was concerned, four key steps including intermolecular alkyne insertion, 1,4-Rh migration, intramolecular addition onto the tethered alkene moiety, and protonolysis were proposed to be involved.



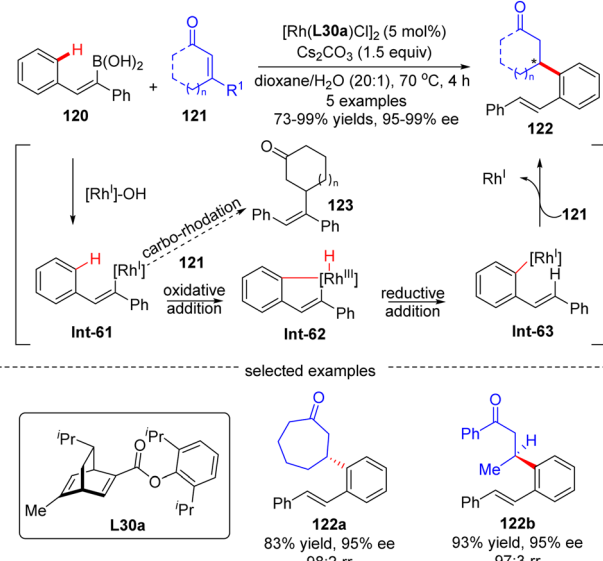
**Scheme 34** Rh(i)-Catalyzed enantioselective addition of sodium tetraarylboration to alkyne-tethered 2-cycloalken-1-ones.

In 2012, Hayashi's group reported a tandem 1,4-Rh migration/1,4-addition process of 2-arylethenylboronic acid **120** to enones **121** by use of chiral ligand **L30a**, a new chiral diene derivative from (R)-phellandrene (Scheme 36).<sup>109</sup> With regard to the variability of the substrates, both cyclic and acyclic enones **121** were tolerated to produce the rearranged products **122** with high yields and excellent regio- and *enantio*-selectivities. The catalytic cycle of this reaction involved a transmetalation to form the 2-phenylethenyl-Rh(i) intermediate **Int-61**, 1,4-Rh migration to give **Int-63**, and enantioselective 1,4-addition onto enones **121** to arrive at the desired products **122**. Density functional theory (DFT) studies indicated that the 1,4-Rh migration proceeded *via* an oxidative addition onto the aryl C–H bond in **Int-61**, leading to a distorted square-pyramidal Rh(III)–H species **Int-62**, and followed by reductive elimination of **Int-62** to afford **Int-63**.

In 2019, by using the chiral diene derivative **L31** with an anthracen-9-yl substituent as a ligand, Darses' group successfully developed an asymmetric arylative cyclization of propargylic malonates **124** with arylboronic acids **125**, giving access to chiral 1-tetralones **126** with a quaternary carbon stereocenter *via* the desymmetrization of the malonate moiety (Scheme 37).<sup>110</sup> This reaction involved a regioselective alkyne insertion, an alkenyl-to-aryl 1,4-Rh migration and an acylation process. The 2,4-bis(trifluoromethyl)phenyl substituent on propargyl malonates **124** played an important role in controlling the regioselectivity of alkyne insertion (>99:1). Alkyl-, alkoxyl, and amino-substituted alkynylmalonates were all competent substrates to generate the desired 1-tetralones **126** in favorable yields (up to 96%) and enantioselectivities (up to 96% ee). Of note, one enantioselective variant of 1-tetralone was also prepared from bis(2,2,2-trifluoroethyl)-malonate by Lam's group under the catalysis of  $[\text{RhCl}(\text{C}_2\text{H}_4)_2]_2$  and (R)-MeO-BIHEP.<sup>111</sup>



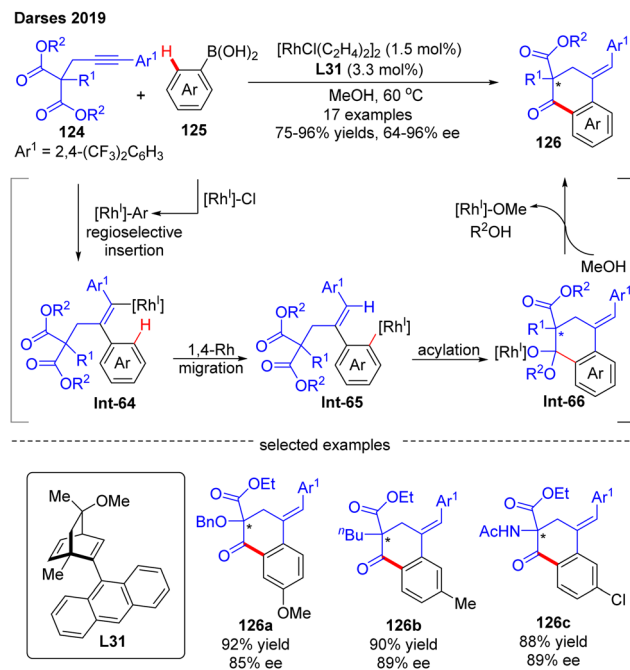
**Scheme 35** Rh(i)-Catalyzed asymmetric indane synthesis from 1,4-enynes and arylboronic acids.



**Scheme 36** Rh(i)-Catalyzed 1,4-migration/1,4-addition of 2-arylethenylboronic acid to enones.

In 2020, Lam's group developed a Rh(i)-catalyzed asymmetric arylation/annulation reaction of 2-propargyl-1,3-diketones **127** with arylboronic acids **128** involving an alkenyl-to-aryl 1,4-Rh migration as the key step, thus giving access to densely functionalized polycarbocycles **129** containing two contiguous quaternary stereogenic centers (Scheme 38).<sup>112</sup> By the use of the  $[\text{RhCl}(\text{C}_2\text{H}_4)_2]_2$  catalyst combined with (S)-DTBM-Segphos ligand *ent*-**L9d**, the desired products **129** were achieved in excellent enantioselectivities (up to 99% ee) and diastereoselectivities (in most cases  $\text{dr} > 19:1$ ). A broad range of functional groups on both reaction partners were well tolerated

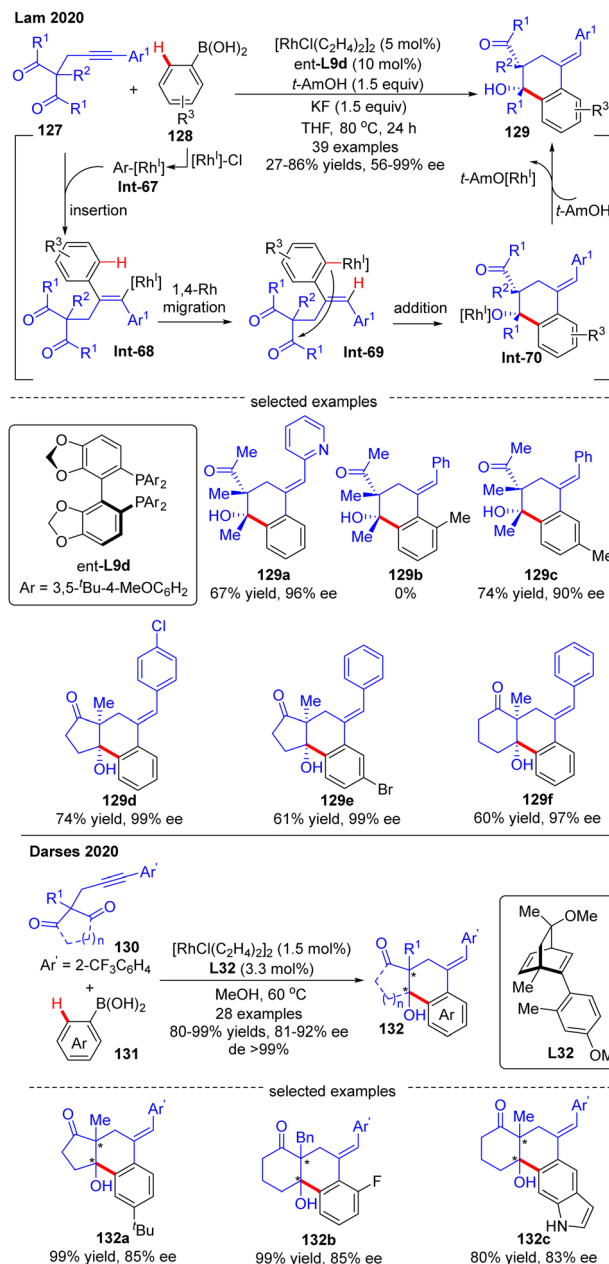




Scheme 37 Rh(i)-Catalyzed arylative cyclization of propargylic malonates with arylboronic acids.

regardless of the electronic effect, whereas the steric factor played a critical role in the reactivity as reflected by the failure of 2-methylphenylboronic acid as a substrate (**129b**). It was also found that 3-substituted arylboronic acids favored affording the less sterically hindered products (**129c**). When cyclic 1,3-diketones were used as a substrate, favorable results were also achieved to give **129d–f** in 60–74% yields and 97–99% ee. It was hypothesized that this reaction might experience a transmetalation/migratory insertion/1,4-Rh migration/1,2-addition sequence. The similar transformation between 1,3-diketones and aryl boronic acids was also realized by Darses and co-workers by use of chiral diene **L32** as a ligand, providing straightforward access to 1-tetralols **132** containing two contiguous quaternary stereogenic centers in good enantioselectivities (81–92% ee) and diastereoselectivities (>99% de) (Scheme 38).<sup>113</sup> Diverse 2-propargyl-1,3-diketones including cyclic and acyclic substrates with various functional groups were all well tolerated in this reaction. It is worth mentioning that the 2-trifluoromethyl-phenyl substituent (Ar') on the alkyne moiety of **130** was essential to achieve high regioselectivity for alkyne insertion.

Darses's research group also investigated the cascade reactions of enyne derivatives with arylboronic acids by taking advantage of asymmetric catalysis with Rh(i)/chiral diene complexes. In 2017, they disclosed the preparation of various 7-membered chiral azepane **135** in moderate to high yields (36–93%) and good enantiomeric excess (86–97%) by using the *N*-tethered alkyne enoates **133** and aryl boronic acids **134** as substrates and chiral diene **L32** or **L33** as a ligand (Scheme 39).<sup>114</sup> This reaction displayed good functional group tolerance. Shortly after, Darses and co-workers further developed an efficient access to chiral tetrahydrofurans **138** and tetrahydrobenzo[*d*]oxepines **139** in decent stereo-control from



Scheme 38 Rh(i)-Catalyzed arylative cyclization of 2-propargyl-1,3-diketones with arylboronic acids.

simple *O*-tethered alkyne enoates **136**.<sup>115</sup> When the R<sup>1</sup> substituent in **136** was methyl, the chiral 5-membered tetrahydrofurans **138** were obtained, whereas the enantioenriched 7-membered tetrahydrobenzo[*d*]oxepines **139** was produced when the R<sup>1</sup> substituent was aryl. The differed product structures were ascribed to a switch of the regioselectivity of alkyne insertion by the alkyne substituent, suggesting that the regioselectivity of the alkyne insertion may be impacted by the steric and electronic properties of R<sup>1</sup> substituents.<sup>116</sup>

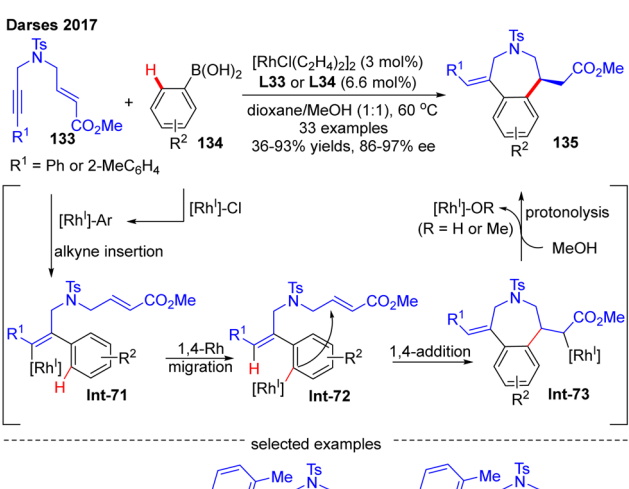
**4.1.2 C(sp<sup>2</sup>)-H functionalization via alkyl-to-aryl 1,4-Rh migration.** In 2007, Murakami's group developed a Rh(i)-catalyzed cascade reaction of 3-(2-hydroxyphenyl)-cyclobutanones **140** with electron-deficient alkenes **141** via an alkyl-to-aryl 1,4-Rh

migration (Scheme 40).<sup>117</sup> Using  $[\text{RhOH}(\text{cod})]_2$  as a catalyst and  $(R)$ -Tol-BINAP L7a as a chiral ligand, several 4,4-disubstituted 3,4-dihydrocoumarins 142 were obtained in high yields (65–93%) and enantioselectivities (91–97% ee). It was proposed that this cascade reaction might involve a carbonyl addition, a ring opening *via*  $\beta$ -C elimination, a 1,4-Rh migration, and an intermolecular 1,4-addition. Specifically, rhodium aryloxide Int-74 was first generated from 140 with  $[\text{RhOH}(\text{cod})]_2$ . Intramolecular addition onto the carbonyl group in Int-74 happened to produce the rhodium cyclobutanolate Int-75, which readily proceeded  $\beta$ -C elimination, forging ring-opening alkyl rhodium species Int-76. This step was believed as the stereochemistry-determining step of this reaction. Afterwards, the arylrhodium species Int-77 was then generated from Int-76 *via* a 1,4-rhodium migration process. A final intermolecular 1,4-addition of Int-77 onto electron-deficient alkenes 141 arrived at the enantioenriched 3,4-dihydrocoumarins 142.

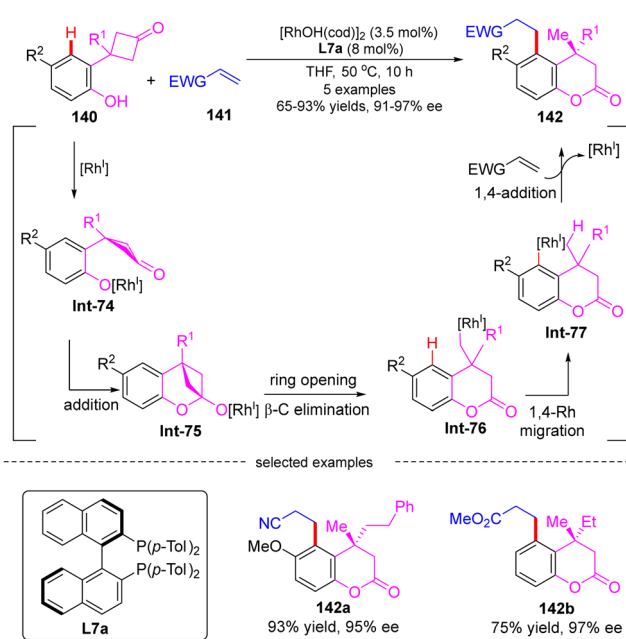
In 2009, Cramer and co-workers successfully prepared enantioenriched 1-indanols 144 from cyclobutanols 143 under the catalysis of  $[\text{RhOH}(\text{cod})]_2$  (Scheme 41).<sup>118</sup> When 3-aryl-3'-methyl-cyclobutanols were used as substrates, Josiphos-type ligand L19 with an electron-withdrawing trifluoromethyl group

demonstrated as the optimal, providing products 144a and 144b as a single stereoisomer with decent yields and stereocontrol. Interestingly, when the 3'-position of cyclobutanols was not methyl, diastereoisomers existed and the chiral ligand had a great influence on the diastereomeric ratios, as reflected by the increased diastereoselectivity by taking advantage of the difluorophos ligand *ent*-L10 (144c, 20:1 vs. 1.2:1 with L19 and *ent*-L10, respectively). As illustrated in Scheme 41, the reaction was proposed to be initiated by the formation of the rhodium cyclobutanolate Int-78 *via* deprotonation of 143. Fragmentation of the cyclobutane ring in Int-78 occurred to form the alkyl rhodium species Int-79 *via*  $\beta$ -C elimination. Following a 1,4-Rh migration process of Int-79, the aryl rhodium species Int-80 bearing one quaternary carbon was produced, which was further turned into Int-81 containing two quaternary carbons through intramolecular 1,2-addition. The desired product 1-indanols 144 was finally released by protonation of Int-81. A similar approach to stereoselective restructuring of 3-arylcyclobutanols 145 into 1-indanols 146 was also reported by Murakami's group,<sup>119</sup> and the underlying mechanism was systematically studied by Dang's group with DFT calculations in 2014.<sup>120</sup> The results showed that the stereoselectivity of this reaction was contributed by three main factors including the relative stability of  $\beta$ -C elimination product, the kinetic feasibilities of 1,4-Rh migration, and the relative free energies of  $\text{C}=\text{O}$  insertion step.

As an extension of the above-described transformation, in 2010, Cramer's group further achieved the asymmetric synthesis of indanones 148 bearing a quaternary stereogenic center from 1-arylcyclobutanols 147 (Scheme 42).<sup>121</sup> Similar to the previous transformations, rhodium alkoxide Int-85 was also generated in this reaction through a four-step sequence

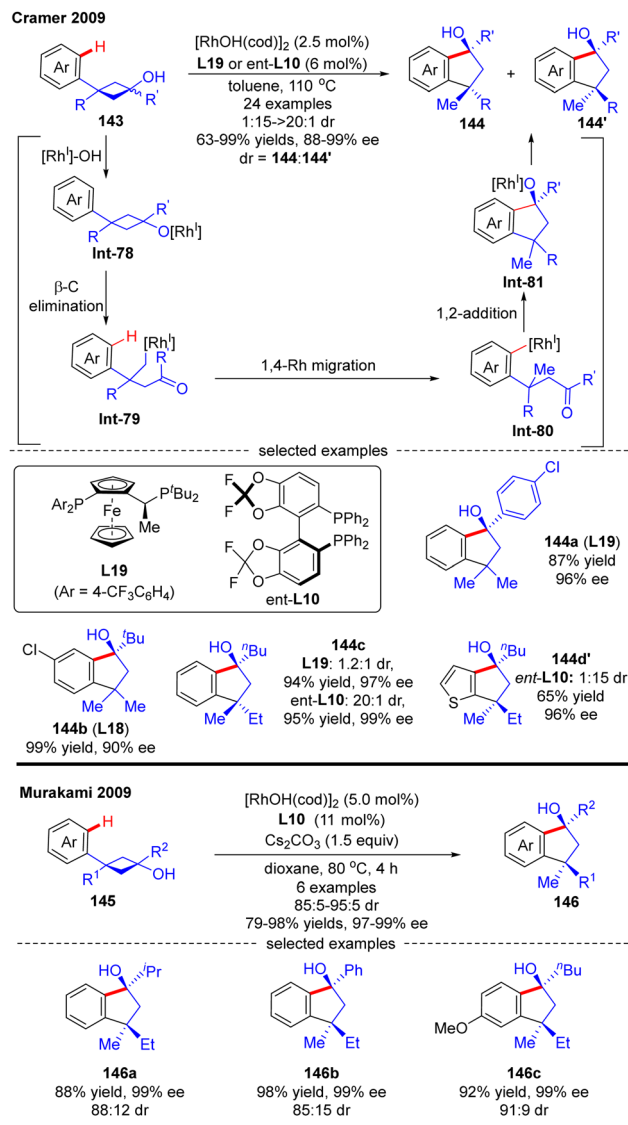


Scheme 39 Rh(I)-Catalyzed arylative cyclization of *N*- or *O*-tethered alkyne enoates with arylboronic acids.



Scheme 40 Rh(I)-Catalyzed cascade reaction of 3-(2-hydroxyphenyl)cyclobutanones with electron-deficient alkenes.





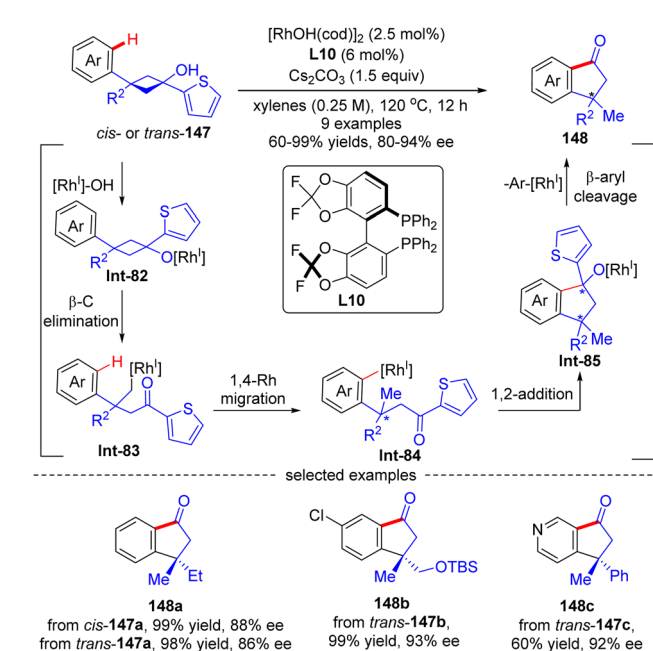
**Scheme 41** Rh(i)-Catalyzed asymmetric synthesis of 1-indanols from 3-arylcyclobutanols.

comprising Rh-catalyzed deprotonation of 1-arylcyclobutanols **147**, cyclobutane fragmentation *via*  $\beta$ -C elimination, alkyl-to-aryl 1,4-Rh migration, and intramolecular 1,2-addition. Next, by contrast to the direct protonolysis in previous transformations, herein **Int-85** underwent a further  $\beta$ -aryl cleavage, leading to indanones **148** with a quaternary carbon center. The aryl substituent on prototype cyclobutanols **147** had a great impact on the reaction pathway of **Int-85**, and the 2-thienyl substituent performed the best to selectively furnish indanones **148** *via*  $\beta$ -aryl cleavage instead of indanols *via* direct protonation. This reaction tolerated a broad range of functional groups, giving the corresponding indanones **148** in 60–99% yields and 80–94% ee. Notably, the geometry of substrates **147** revealed minimal effect on the stereo-control of the desired products (**148a**).

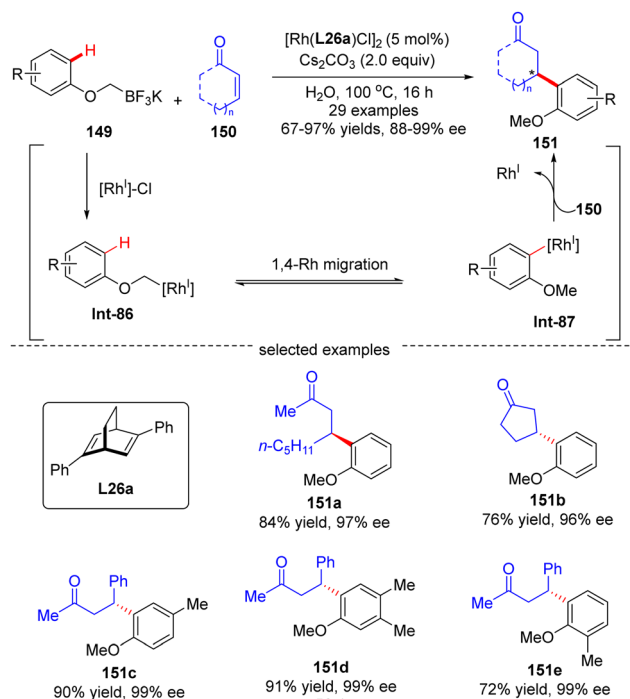
In 2016, Hayashi's group further disclosed a sequential 1,4-Rh migration/arylation reaction of enones **150** with potassium

aryloxymethyltrifluoroborates **149** to yield  $\beta$ -(2-methoxyaryl)-substituted ketones **151** in high yields (67–97%) and excellent enantioselectivities (88–99% ee) *via* asymmetric Rh(i)/diene catalysis (Scheme 43).<sup>122</sup> Both cyclic and linear enones displayed good compatibility. The mechanistic investigation suggested that this reaction involved an alkyl-to-aryl 1,4-Rh migration of aryloxymethyl-Rh intermediate **Int-86**, which forged 2-methoxyaryl-Rh species **Int-87**. This 1,4-Rh migration between C(sp<sup>3</sup>)-H and C(sp<sup>2</sup>)-H was reversible as revealed by the deuterium-labeling studies, and C–H bond cleavage was not the turnover-limiting step. Notably, the regioselectivity for 1,4-Rh migration was impacted by the steric factor, as the less hindered isomer (**151d**) was preferably formed.

**4.1.3 C(sp<sup>2</sup>)-H functionalization *via* aryl-to-alkenyl 1,4-Rh migration.** Aside from the intensively studied alkenyl-to-aryl and alkyl-to-aryl 1,4-Rh migration process, a novel aryl-to-alkenyl 1,4-Rh migration process was also developed by Lin and co-workers to effect enantioselective C(sp<sup>2</sup>)-H functionalization. In 2019, they reported a Rh(i)/BINAP-catalyzed asymmetric alkenylation of enones **153** with 2-ethenyl-arylboronic acids **152**, providing facile access to a wide range of  $\beta$ -alkenylated ketones **154** in high yields (65–99%) and excellent enantiomeric excess (70–99% ee) (Scheme 44).<sup>123</sup> In addition to enones, cyclic aldimines **156** were also compatible with this strategy to prepare a set of chiral allylic sulfonamides **157** by employing (S)-difluorophos **L10** as a chiral ligand. The key to the success of this reaction relied on a highly efficient aryl-to-alkenyl 1,4-Rh migration, which offered a new mode to prepare stereodefined alkenyl-rhodium species **Int-90**. DFT calculations revealed that the aryl-to-alkenyl 1,4-Rh migration was a kinetically favored process, comprising a C–H oxidative addition to form distorted Rh–H species **Int-89** and follow-up reductive



**Scheme 42** Rh(i)-Catalyzed asymmetric synthesis of indanones from 1-(2-thienyl)cyclobutanols.



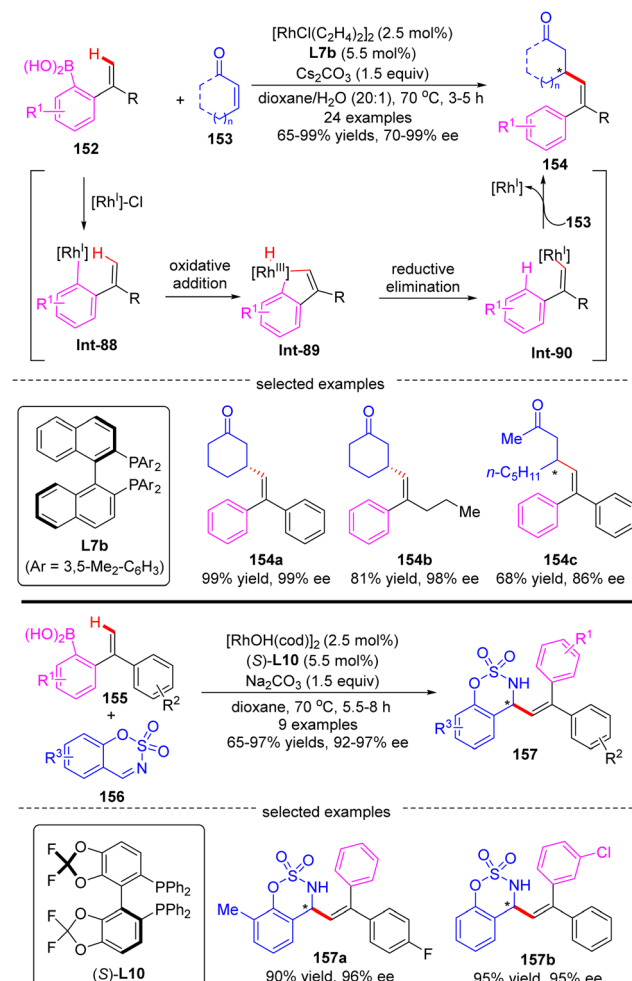
**Scheme 43** Rh(i)-Catalyzed conjugate arylation of enones with potassium aryloxymethyltrifluoroborates.

elimination to generate a stereodefined (*E*)-alkenylrhodium intermediate **Int-90**.

#### 4.2 C(sp<sup>3</sup>)-H functionalization *via* 1,4-Rh migration

In 2014, Lam's group described a facile synthesis of chiral homoallylic sulfonamide **160** from 5-membered cyclic imine **158** and potassium prenyltrifluoroborate **159** *via* a Rh(i)/diene asymmetric catalysis (Scheme 45).<sup>124</sup> Allyl-Rh species **Int-91** was first generated through transmetalation of potassium prenyltrifluoroborate **159** with [Rh]-Cl. With the less reactive saccharin-derived imine **158**, it is disfavored to forge the reverse prenylation product **160'** with sterical congestion *via* direct addition of **Int-91** to the imine substrate as per the previous report.<sup>125</sup> Instead, an allyl-to-allyl 1,4-Rh migration occurred, furnishing another alkyl-Rh species **Int-92**. Finally, nucleophilic addition of **Int-92** onto cyclic imine **158** proceeded to arrive at the desired homoallylic sulfonamide **160** as the major isomer in decent yield and excellent *enantio*-control. Notwithstanding, the minor isomer **160'** was also observed *via* the direct addition of **Int-91** onto cyclic imine **158**. It is worth mentioning that the 1,4-Rh migration was a reversible process and the steric hindrance of allyltrifluoroborates may promote the following isomerization of allyl-Rh species **Int-94** to afford **Int-95**. Indeed, with the more sterically hindered allyltrifluoroborates **162** and chiral ligand *ent*-**L26a**, homoallylic sulfonamide **163** was produced as a single isomer *via* nucleophilic addition of **Int-93** onto more reactive aldimine **161**.

In 2017, Lam's group further reported an enantioselective Rh(i)-catalyzed three-component coupling of 1,3-enynes **164**, arylboronic acids **165** and cyclic aldimines **166** (Scheme 46).<sup>126</sup> The



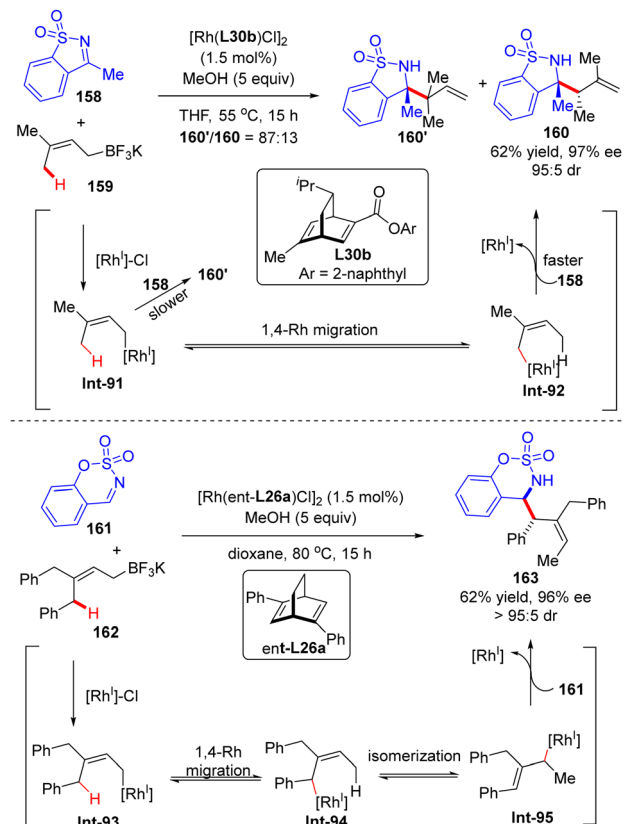
**Scheme 44** Rh(i)-Catalyzed alkenylation of enones and cyclic imines with 2-ethenyl-arylboronic acids.

efficient catalytic system of [RhCl(C<sub>2</sub>H<sub>4</sub>)<sub>2</sub>]/chiral tetrafluorobenzobarrelene **L37** enabled a straightforward access to a diverse of branched homoallylic sulfonamides **167** bearing tertiary or quaternary carbon stereogenic centers in decent yields (33–77%), high enantioselectivities (up to 99% ee) and excellent diastereoselectivities (in most cases >19:1). The underlying mechanism was proposed as exhibited in Scheme 46. First, transmetalation of arylboronic acid **165** with *in situ* generated [Rh]-Cl produced the arylrhodium species **Int-96**. Then, the migratory insertion of **Int-96** across 1,3-enynes **164** occurred, furnishing alkenylrhodium species **Int-97**. Afterwards, **Int-97** underwent a reverse alkenyl-to-allyl 1,4-Rh migration to produce **Int-98**, which was considered as the key step of this reaction. Subsequent intermolecular nucleophilic addition of **Int-98** to cyclic imine **166** proceeded to form **Int-99**. The final protonolysis of **Int-99** released the homoallylated product **167** with the regeneration of the rhodium complex.

## 5. Conclusion and outlook

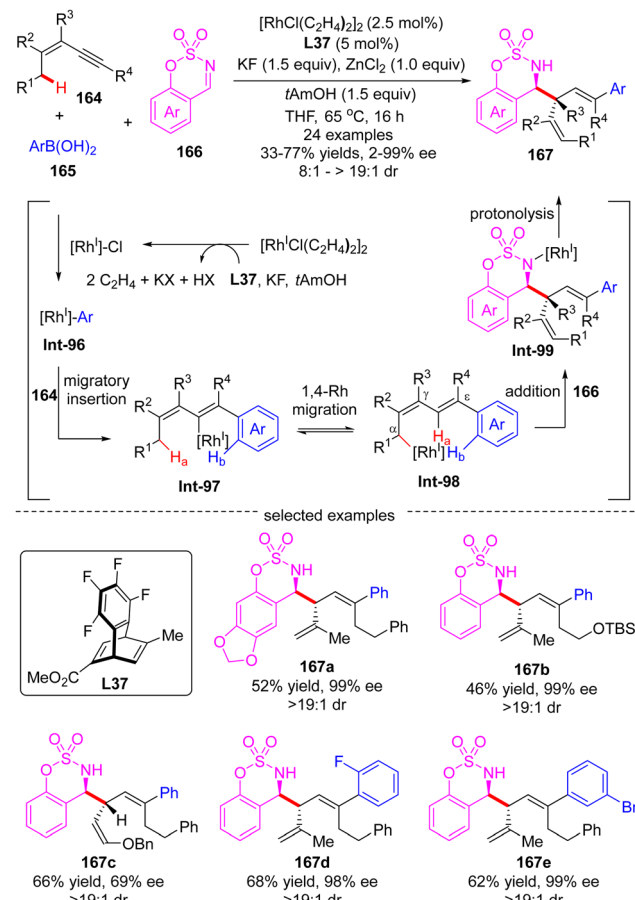
Among the various rhodium complexes, Rh(i) has mainly been utilized for the direct functionalization of C–H bonds *via*





**Scheme 45** Rh(i)-Catalyzed allylation of cyclic imines with potassium prenyl trifluoroborates.

oxidation addition in both directed and undirected patterns. Although some related reactions could also be effected by other transition metals, Rh(i) catalysis provides the advantage of fine-tuning due to the commercial availability of a diversity of chiral ligands. As illustrated in this review, organic chemists have successfully used Rh(i) catalysis to enable a plethora of asymmetric C–H functionalization reactions including arylation, alkylation, and silylation, which serve as a versatile and efficient synthetic complement to Rh(ii) and Rh(iii) catalysis. Despite these impressive progresses, several major limitations still remain in the realm of Rh(i)-catalyzed C–H activation for asymmetric functionalization, such as the requisite of directing group for C–H functionalization, the confine of unactivated C(sp<sup>3</sup>)–H functionalization into an intramolecular fashion, the lack of applications in forging carbon–heteroatom bonds (*e.g.*, C–O, C–N, C–S, C–X, and C–P) aside from C–Si bonds (partially owing to the competing coordination of heteroatoms with the chiral ligands), and the elusive 1,4-Rh migration to general C(sp<sup>3</sup>)–H bonds. Therefore, it is still of immense demand to devote more efforts to developing transient directing group strategy or non-directed Rh(i)-catalyzed asymmetric C–H functionalization, uncovering intermolecular asymmetric silylation and unactivated C(sp<sup>3</sup>)–H functionalization reactions, and designing novel chiral ligands to circumvent the catalyst poison issue by heteroatoms. More importantly, a deeper understanding of the mechanism in Rh(i)-catalyzed asymmetric C–H



**Scheme 46** Rh(i)-Catalyzed three-component allylation of cyclic imines with arylboronic acids and 1,3-enynes.

functionalization reactions is highly desirable to facilitate the rational design of new asymmetric reactions. Additionally, the synthetic implementation in the late-stage functionalization of natural products or other complex molecules also needs to be validated. As such, one can forecast that more novel Rh(i)-catalyzed asymmetric C–H functionalization reactions will be well-designed and applicable in the near future.

## Conflicts of interest

There are no conflicts to declare.

## Acknowledgements

We are grateful to the Basic Research Program of Jiangsu Province (BK20220408), the National Natural Science Foundation of China (22001260), Guangdong Basic and Applied Basic Research Foundation (2021A1515010016), and Shenzhen Science and Technology Innovation Committee (JCYJ20210324101810028, JCYJ20220818101601004, JCYJ20220818095801004).



## References

- 1 E. J. Corey and X. M. Cheng, *The Logic of Chemical Synthesis*, Wiley, New York, 1989.
- 2 T. Hudlicky and J. W. Reed, *The Way of Synthesis: Evolution of Design and Methods for Natural Products*, Wiley-VCH, Weinheim, Germany, 2007.
- 3 E. J. Corey and L. Kürti, *Enantioselective Chemical Synthesis: Methods, Logic, and Practice*, ed. E. J. Corey and L. Kürti, Direct Book Publishing, Dallas, TX, 2010.
- 4 W. R. Gutekunst and P. S. Baran, *Chem. Soc. Rev.*, 2011, **40**, 1976–1991.
- 5 L. McMurray, F. O'Hara and M. J. Gaunt, *Chem. Soc. Rev.*, 2011, **40**, 1885–1898.
- 6 J. Yamaguchi, A. D. Yamaguchi and K. Itami, *Angew. Chem., Int. Ed.*, 2012, **51**, 8960–9009.
- 7 Y. Qiu and S. Gao, *Nat. Prod. Rep.*, 2016, **33**, 562–581.
- 8 D. J. Abrams, P. A. Provencher and E. J. Sorensen, *Chem. Soc. Rev.*, 2018, **47**, 8925–8967.
- 9 R. Giri, B.-F. Shi, K. M. Engle, N. Maugel and J.-Q. Yu, *Chem. Soc. Rev.*, 2009, **38**, 3242–3272.
- 10 C. Zheng and S.-L. You, *RSC Adv.*, 2014, **4**, 6173–6214.
- 11 D.-Y. Zhu, P. Chen and J.-B. Xia, *ChemCatChem*, 2016, **8**, 68–73.
- 12 Z. Dong, Z. Ren, S. J. Thompson, Y. Xu and G. Dong, *Chem. Rev.*, 2017, **117**, 9333–9403.
- 13 C. G. Newton, S.-G. Wang, C. C. Oliveira and N. Cramer, *Chem. Rev.*, 2017, **117**, 8908–8976.
- 14 Z. Chen, M.-Y. Rong, J. Nie, X.-F. Zhu, B.-F. Shi and J.-A. Ma, *Chem. Soc. Rev.*, 2019, **48**, 4921–4942.
- 15 J. Diesel and N. Cramer, *ACS Catal.*, 2019, **9**, 9164–9177.
- 16 G. Liao, T. Zhou, Q.-J. Yao and B.-F. Shi, *Chem. Commun.*, 2019, **55**, 8514–8523.
- 17 R. Wang, Y. Luan and M. Ye, *Chin. J. Chem.*, 2019, **37**, 720–743.
- 18 Ł. Woźniak and N. Cramer, *Trends Chem.*, 2019, **1**, 471–484.
- 19 T. K. Achar, S. Maiti, S. Jana and D. Maiti, *ACS Catal.*, 2020, **10**, 13748–13793.
- 20 C.-X. Liu, Q. Gu and S.-L. You, *Trends Chem.*, 2020, **2**, 737–749.
- 21 J. Thongpaen, R. Manguin and O. Baslé, *Angew. Chem., Int. Ed.*, 2020, **59**, 10242–10251.
- 22 Ł. Woźniak, J.-F. Tan, Q.-H. Nguyen, A. Madron du Vigné, V. Smal, Y.-X. Cao and N. Cramer, *Chem. Rev.*, 2020, **120**, 10516–10543.
- 23 K. Yang, M. Song, H. Liu and H. Ge, *Chem. Sci.*, 2020, **11**, 12616–12632.
- 24 X.-L. Liu, L.-B. Jiang, M.-P. Luo, Z. Ren and S.-G. Wang, *Org. Chem. Front.*, 2022, **9**, 265–280.
- 25 C. Pan, S.-Y. Yin, Q. Gu and S.-L. You, *Org. Biomol. Chem.*, 2021, **19**, 7264–7275.
- 26 J. Wencel-Delord and F. Colobert, *Chem. – Eur. J.*, 2013, **19**, 14010–14017.
- 27 T. Yoshino, S. Satake and S. Matsunaga, *Chem. – Eur. J.*, 2020, **26**, 7346–7357.
- 28 M. I. Lapuh, S. Mazeh and T. Basset, *ACS Catal.*, 2020, **10**, 12898–12919.
- 29 G. Liao, T. Zhang, Z.-K. Lin and B.-F. Shi, *Angew. Chem., Int. Ed.*, 2020, **59**, 19773–19786.
- 30 B.-F. S. Ya-Lan Feng, *Chin. J. Org. Chem.*, 2021, **41**, 3753–3770.
- 31 Q. Zhang and B.-F. Shi, *Acc. Chem. Res.*, 2021, **54**, 2750–2763.
- 32 S. Motevali, Y. Sokeirik and A. Ghanem, *Eur. J. Org. Chem.*, 2016, 1459–1475.
- 33 W.-W. Chen and M.-H. Xu, *Org. Biomol. Chem.*, 2017, **15**, 1029–1050.
- 34 X. Qi, Y. Li, R. Bai and Y. Lan, *Acc. Chem. Res.*, 2017, **50**, 2799–2808.
- 35 E. A. Trifonova, N. M. Ankudinov, A. A. Mikhaylov, D. A. Chusov, Y. V. Nelyubina and D. S. Perekalin, *Angew. Chem., Int. Ed.*, 2018, **57**, 7714–7718.
- 36 *Rhodium Catalysis in Organic Synthesis*, ed. K. Tanaka, Wiley-VCH, Weinheim, Germany, 2019.
- 37 S. Rej and N. Chatani, *Angew. Chem., Int. Ed.*, 2019, **58**, 8304–8329.
- 38 B. Ye and N. Cramer, *Acc. Chem. Res.*, 2015, **48**, 1308–1318.
- 39 J. Mas-Roselló, A. G. Herraiz, B. Audic, A. Laverny and N. Cramer, *Angew. Chem., Int. Ed.*, 2021, **60**, 13198–13224.
- 40 Y. Cao and K. G. M. Kou, Rhodium-Catalyzed Heterocycle Synthesis by C–H Functionalization, *Handbook of C–H Functionalization*, 2022, pp. 1–39.
- 41 N. Chatani, Rhodium-Catalyzed C(sp<sup>3</sup>)–H Functionalization, *Handbook of C–H Functionalization*, 2022, pp. 1–34.
- 42 V. Hanchate, M. S. Sherikar, A. Kumar and K. R. Prabhu, Rh-Catalyzed C–H Functionalization with Alkene, *Handbook of C–H Functionalization*, 2022, pp. 1–44.
- 43 S. Mahato, W. Sarkar, K. Naskar and I. Deb, Rhodium-Catalyzed C–H Functionalization to Construct Annulated Molecules, *Handbook of C–H Functionalization*, 2022, pp. 1–39.
- 44 A. Singh and C. M. R. Volla, Rh-Catalyzed C–H Functionalization with Allenes, *Handbook of C–H Functionalization*, 2022, pp. 1–29.
- 45 C.-X. Liu, S.-Y. Yin, F. Zhao, H. Yang, Z. Feng, Q. Gu and S.-L. You, *Chem. Rev.*, 2023, **123**, 10079–10134.
- 46 R. H. Crabtree, *J. Chem. Soc., Dalton Trans.*, 2001, **2001**, 2437–2450.
- 47 A. R. Dick and M. S. Sanford, *Tetrahedron*, 2006, **62**, 2439–2463.
- 48 C. G. Newton and N. Cramer, Chiral Cp Ligands for Rhodium(III)-Catalyzed Asymmetric Carbon–Hydrogen Bond Functionalization, in *Rhodium Catalysis in Organic Synthesis*, ed. K. Tanaka, Wiley-VCH, Weinheim, Germany, 2019, pp. 629–644.
- 49 F. Romanov-Michailidis, E. J. T. Phipps and T. Rovis, Sterically and Electronically Tuned Cp Ligands for Rhodium(III)-Catalyzed Carbon–Hydrogen Bond Functionalization, in *Rhodium Catalysis in Organic Synthesis*, ed. K. Tanaka, Wiley-VCH, Weinheim, Germany, 2019, pp. 593–628.
- 50 T. Satoh and M. Miura, Rhodium(III)-Catalyzed Annulative Carbon–Hydrogen Bond Functionalization, in *Rhodium*



*Catalysis in Organic Synthesis*, ed. K. Tanaka, Wiley-VCH, Weinheim, Germany, 2019, pp. 487–519.

51 F. Xie and X. Li, Rhodium(III)-Catalyzed Non-annulative Carbon–Hydrogen Bond Functionalization, in *Rhodium Catalysis in Organic Synthesis*, ed. K. Tanaka, Wiley-VCH, Weinheim, Germany, 2019, pp. 521–592.

52 T. G. Driver, Rhodium(II)-Catalyzed Nitrogen-Atom Transfer for Oxidation of Aliphatic C–H Bonds, in *Rhodium Catalysis in Organic Synthesis*, ed. K. Tanaka, Wiley-VCH, Weinheim, Germany, 2019, pp. 373–432.

53 T. Miura and M. Murakami, Reactions of  $\alpha$ -Imino Rhodium(II) Carbene Complexes Generated from N-Sulfonyl-1,2,3-Triazoles, in *Rhodium Catalysis in Organic Synthesis*, ed. K. Tanaka, Wiley-VCH, Weinheim, Germany, 2019, pp. 449–470.

54 S. M. Wilkerson-Hill and H. M. L. Davies, Rhodium(II) Tetracarboxylate-Catalyzed Enantioselective C–H Functionalization Reactions, in *Rhodium Catalysis in Organic Synthesis*, ed. K. Tanaka, Wiley-VCH, Weinheim, Germany, 2019, pp. 341–372.

55 Z. Chen and V. M. Dong, Rhodium(I)-Catalyzed Hydroformylation and Hydroamination, in *Rhodium Catalysis in Organic Synthesis*, ed. K. Tanaka, Wiley-VCH, Weinheim, Germany, 2019, pp. 49–62.

56 M. Fernández and M. C. Willis, Rhodium(I)-Catalyzed Hydroacylation, in *Rhodium Catalysis in Organic Synthesis*, ed. K. Tanaka, Wiley-VCH, Weinheim, Germany, 2019, pp. 63–84.

57 N. Fujii, F. Kakiuchi, A. Yamada, N. Chatani and S. Murai, *Chem. Lett.*, 1997, 425–426.

58 R. K. Thalji, J. A. Ellman and R. G. Bergman, *J. Am. Chem. Soc.*, 2004, **126**, 7192–7193.

59 H. Harada, R. K. Thalji, R. G. Bergman and J. A. Ellman, *J. Org. Chem.*, 2008, **73**, 6772–6779.

60 R. M. Wilson, R. K. Thalji, R. G. Bergman and J. A. Ellman, *Org. Lett.*, 2006, **8**, 1745–1747.

61 K. Tsuchikama, Y. Kuwata, Y.-K. Tahara, Y. Yoshinami and T. Shibata, *Org. Lett.*, 2007, **9**, 3097–3099.

62 A. S. Tsai, R. M. Wilson, H. Harada, R. G. Bergman and J. A. Ellman, *Chem. Commun.*, 2009, 3910–3912, DOI: [10.1039/B902878A](https://doi.org/10.1039/B902878A).

63 S. H. Wiedemann, J. C. Lewis, J. A. Ellman and R. G. Bergman, *J. Am. Chem. Soc.*, 2006, **128**, 2452–2462.

64 Z.-M. Sun, S.-P. Chen and P. Zhao, *Chem. – Eur. J.*, 2010, **16**, 2619–2627.

65 D. N. Tran and N. Cramer, *Angew. Chem., Int. Ed.*, 2011, **50**, 11098–11102.

66 D. N. Tran and N. Cramer, *Angew. Chem., Int. Ed.*, 2010, **49**, 8181–8184.

67 D. N. Tran and N. Cramer, *Angew. Chem., Int. Ed.*, 2013, **52**, 10630–10634.

68 M. Tsutsui, M. Hancock, J. Ariyoshi and M. N. Levy, *Angew. Chem., Int. Ed. Engl.*, 1969, **8**, 410–420.

69 C. M. Filloux and T. Rovis, *J. Am. Chem. Soc.*, 2015, **137**, 508–517.

70 F. Kakiuchi, P. Le Gendre, A. Yamada, H. Ohtaki and S. Murai, *Tetrahedron: Asymmetry*, 2000, **11**, 2647–2651.

71 Q. Wang, Z.-J. Cai, C.-X. Liu, Q. Gu and S.-L. You, *J. Am. Chem. Soc.*, 2019, **141**, 9504–9510.

72 Z.-J. Cai, C.-X. Liu, Q. Wang, Q. Gu and S.-L. You, *Nat. Commun.*, 2019, **10**, 4168.

73 C.-X. Liu, Z.-J. Cai, Q. Wang, Z.-J. Wu, Q. Gu and S.-L. You, *CCS Chem.*, 2020, **2**, 642–651.

74 C.-X. Liu, F. Zhao, Z. Feng, Q. Wang, Q. Gu and S.-L. You, *Nat. Syn.*, 2023, **2**, 49–57.

75 C.-X. Liu, P.-P. Xie, F. Zhao, Q. Wang, Z. Feng, H. Wang, C. Zheng and S.-L. You, *J. Am. Chem. Soc.*, 2023, **145**, 4765–4773.

76 C.-X. Liu, F. Zhao, Q. Gu and S.-L. You, *ACS Cent. Sci.*, 2023, **9**, 2036–2043.

77 Y. Kuninobu, K. Yamauchi, N. Tamura, T. Seiki and K. Takai, *Angew. Chem., Int. Ed.*, 2013, **52**, 1520–1522.

78 Y. Kuninobu, K. Yamauchi, N. Tamura, T. Seiki and K. Takai, *Angew. Chem., Int. Ed.*, 2016, **55**, 1948.

79 M. Murai, Y. Takeuchi, K. Yamauchi, Y. Kuninobu and K. Takai, *Chem. – Eur. J.*, 2016, **22**, 6048–6058.

80 Q.-W. Zhang, K. An, L.-C. Liu, Y. Yue and W. He, *Angew. Chem., Int. Ed.*, 2015, **54**, 6918–6921.

81 M. Murai, K. Matsumoto, Y. Takeuchi and K. Takai, *Org. Lett.*, 2015, **17**, 3102–3105.

82 M. Murai, K. Matsumoto, Y. Takeuchi and K. Takai, *Org. Lett.*, 2016, **18**, 3041.

83 T. Shibata, T. Shizuno and T. Sasaki, *Chem. Commun.*, 2015, **51**, 7802–7804.

84 D. Mu, W. Yuan, S. Chen, N. Wang, B. Yang, L. You, B. Zu, P. Yu and C. He, *J. Am. Chem. Soc.*, 2020, **142**, 13459–13468.

85 W. Ma, L.-C. Liu, K. An, T. He and W. He, *Angew. Chem., Int. Ed.*, 2021, **60**, 4245–4251.

86 W. Yuan, L. You, W. Lin, J. Ke, Y. Li and C. He, *Org. Lett.*, 2021, **23**, 1367–1372.

87 S. Chen, D. Mu, P.-L. Mai, J. Ke, Y. Li and C. He, *Nat. Commun.*, 2021, **12**, 1249.

88 Q.-W. Zhang, K. An, L.-C. Liu, Q. Zhang, H. Guo and W. He, *Angew. Chem., Int. Ed.*, 2017, **56**, 1125–1129.

89 K. An, W. Ma, L.-C. Liu, T. He, G. Guan, Q.-W. Zhang and W. He, *Nat. Commun.*, 2022, **13**, 847.

90 S. Chen, J. Zhu, J. Ke, Y. Li and C. He, *Angew. Chem., Int. Ed.*, 2022, **61**, e202117820.

91 Q. Li and Z.-X. Yu, *Angew. Chem., Int. Ed.*, 2011, **50**, 2144–2147.

92 Q. Li and Z.-X. Yu, *Organometallics*, 2012, **31**, 5185–5195.

93 J. H. Kim, S. Gressies, M. Boultadakis-Arapinis, C. Daniliuc and F. Glorius, *ACS Catal.*, 2016, **6**, 7652–7656.

94 S. Gressies, F. J. R. Klauck, J. H. Kim, C. G. Daniliuc and F. Glorius, *Angew. Chem., Int. Ed.*, 2018, **57**, 9950–9954.

95 M. Murai, H. Takeshima, H. Morita, Y. Kuninobu and K. Takai, *J. Org. Chem.*, 2015, **80**, 5407–5414.

96 T. Lee and J. F. Hartwig, *Angew. Chem., Int. Ed.*, 2016, **55**, 8723–8727.

97 B. Yang, W. Yang, Y. Guo, L. You and C. He, *Angew. Chem., Int. Ed.*, 2020, **59**, 22217–22222.

98 Y. Guo, M.-M. Liu, X. Zhu, L. Zhu and C. He, *Angew. Chem., Int. Ed.*, 2021, **60**, 13887–13891.



99 R.-T. Guo, Y.-L. Zhang, J.-J. Tian, K.-Y. Zhu and X.-C. Wang, *Org. Lett.*, 2020, **22**, 908–913.

100 D.-X. Zhu, H. Xia, J.-G. Liu, L. W. Chung and M.-H. Xu, *J. Am. Chem. Soc.*, 2021, **143**, 2608–2619.

101 D.-X. Zhu, J.-G. Liu and M.-H. Xu, *J. Am. Chem. Soc.*, 2021, **143**, 8583–8589.

102 B. Liu and M.-H. Xu, *Chin. J. Chem.*, 2021, **39**, 1911–1915.

103 T.-Y. Wang, X.-X. Chen, D.-X. Zhu, L. W. Chung and M.-H. Xu, *Angew. Chem., Int. Ed.*, 2022, **61**, e202207008.

104 D.-X. Zhu and M.-H. Xu, *J. Org. Chem.*, 2023, **88**, 7844–7848.

105 R. Shintani, K. Yashio, T. Nakamura, K. Okamoto, T. Shimada and T. Hayashi, *J. Am. Chem. Soc.*, 2006, **128**, 2772–2773.

106 R. Shintani, K. Takatsu and T. Hayashi, *Angew. Chem., Int. Ed.*, 2007, **46**, 3735–3737.

107 R. Shintani, S. Isobe, M. Takeda and T. Hayashi, *Angew. Chem., Int. Ed.*, 2010, **49**, 3795–3798.

108 T. Matsuda and S. Watanuki, *Org. Biomol. Chem.*, 2015, **13**, 702–705.

109 K. Sasaki, T. Nishimura, R. Shintani, E. A. B. Kantichev and T. Hayashi, *Chem. Sci.*, 2012, **3**, 1278–1283.

110 A. Selmani and S. Darses, *Org. Lett.*, 2019, **21**, 8122–8126.

111 L. O'Brien, S. N. Karad, W. Lewis and H. W. Lam, *Chem. Commun.*, 2019, **55**, 11366–11369.

112 A. Groves, J. Sun, H. R. I. Parke, M. Callingham, S. P. Argent, L. J. Taylor and H. W. Lam, *Chem. Sci.*, 2020, **11**, 2759–2764.

113 A. Selmani and S. Darses, *Org. Lett.*, 2020, **22**, 2681–2686.

114 A. Claraz, F. Serpier and S. Darses, *ACS Catal.*, 2017, **7**, 3410–3413.

115 A. Selmani, F. Serpier and S. Darses, *J. Org. Chem.*, 2019, **84**, 4566–4574.

116 T. Johnson, K.-L. Choo and M. Lautens, *Chem. – Eur. J.*, 2014, **20**, 14194–14197.

117 T. Matsuda, M. Shigeno and M. Murakami, *J. Am. Chem. Soc.*, 2007, **129**, 12086–12087.

118 T. Seiser, O. A. Roth and N. Cramer, *Angew. Chem., Int. Ed.*, 2009, **48**, 6320–6323.

119 M. Shigeno, T. Yamamoto and M. Murakami, *Chem. – Eur. J.*, 2009, **15**, 12929–12931.

120 H. Yu, C. Wang, Y. Yang and Z.-M. Dang, *Chem. – Eur. J.*, 2014, **20**, 3839–3848.

121 T. Seiser, G. Cathomen and N. Cramer, *Synlett*, 2010, 1699–1703.

122 J. Ming and T. Hayashi, *Org. Lett.*, 2016, **18**, 6452–6455.

123 S.-S. Zhang, T.-J. Hu, M.-Y. Li, Y.-K. Song, X.-D. Yang, C.-G. Feng and G.-Q. Lin, *Angew. Chem., Int. Ed.*, 2019, **58**, 3387–3391.

124 H. B. Hepburn and H. W. Lam, *Angew. Chem., Int. Ed.*, 2014, **53**, 11605–11610.

125 Y. Luo, H. B. Hepburn, N. Chotsaeng and H. W. Lam, *Angew. Chem., Int. Ed.*, 2012, **51**, 8309–8313.

126 M. Callingham, B. M. Partridge, W. Lewis and H. W. Lam, *Angew. Chem., Int. Ed.*, 2017, **56**, 16352–16356.

